Joint Uplink-Downlink Transmission Design and Full-Loop Control for Latency-Critical Cyber-Physical Systems

Ling Lyu, *Member, IEEE*, Haitian Liu, Yanpeng Dai, *Member, IEEE*, Nan Cheng, *Senior Member, IEEE*, Cailian Chen, *Senior Member, IEEE*, Xinping Guan, *Fellow, IEEE*, and Xuemin Shen, *Fellow, IEEE*

***Abstract*—With the significant advance of wireless communication technology, more networked control systems are looped via wireless networks. However, the dynamics and uncertainties of wireless channels as well as the limitation of radio resources make it challenging to close all loops at each control step. As the open-loop control will lead to performance deterioration, it is essential to jointly optimize the uplink and downlink transmissions for the full-loop control. In this paper, we analyze the impact of transmission delay in uplink and downlink on the full-loop control performance. We then propose a novel multicast transmission scheme for the latency-critical full-loop control. Accordingly, the uplink-downlink transmission and the full-loop control are jointly considered to minimize the control and communication cost. To effectively solve this mixed integer non-linear programming problem, the original problem is decomposed into the uplink transmission problem and the downlink transmission problem. Alternate resource optimization algorithm and multicast resource allocation algorithm are designed. Simulation results show that the proposed scheme has advantage on reducing both the communication and control cost.**

***Index Terms*—Cyber-physical systems, integrated design of communication and control, latency-critical full-loop control, multicast transmission.**

Received 18 June 2025; revised 9 September 2025; accepted 20 October 2025. Date of publication 28 October 2025; date of current version 11 December 2025. This work was supported in part by the National Natural Science Foundation of China under Grant 62573082, Grant 62571081, and Grant 62002042, in part by the Doctoral Research Startup Funds of Liaoning Province under Grant 2025-BS-0216, and in part by the Fundamental Research Funds for the Central Universities under Grant 3132025259 and Grant 3132025258. Recommended for acceptance by Dr. Zhi Liu. *(Corresponding author: Yanpeng Dai.)*

Ling Lyu and Yanpeng Dai are with the School of Information Science and Technology, Dalian Maritime University, Dalian 116026, China, and also with the State Key Laboratory of Integrated Services Networks, Xidian University, Shaanxi 710071, China (e-mail: linglyu@dlmu.edu.cn; yanpengdai@dlmu.edu.cn).

Haitian Liu is with the School of Information Science and Technology, Dalian Maritime University, Dalian 116026, China (e-mail: liuhaitian2022@dlmu.edu.cn).

Nan Cheng is with the State Key Laboratory of Integrated Services Networks and School of Telecommunications Engineering, Xidian University, Shaanxi 710071, China (e-mail: dr.nan.cheng@ieee.org).

Cailian Chen and Xinping Guan are with the School of Automation and Intelligent Sensing, Shanghai Jiao Tong University, Shanghai 200240, China, also with the State Key Laboratory of Submarine Geoscience, School of Automation and Intelligent Sensing, Shanghai Jiao Tong University, Shanghai 200240, China, also with the Key Laboratory for System Control and Information Processing, Ministry of Education of China, Shanghai 200240, China, and also with the Shanghai Key Laboratory for Perception and Control in Industrial Network Systems, Shanghai 200240, China (e-mail: cailianchen@sjtu.edu.cn; xpguan@sjtu.edu.cn).

Xuemin Shen is with the Department of Electrical and Computer Engineering, University of Waterloo, Waterloo, ON N2L 3G1, Canada (e-mail: sshen@uwaterloo.ca).

Digital Object Identifier 10.1109/TNSE.2025.3626216

I. Introduction

With the significant advance of communication technology, an increasing number of factory devices are being interconnected via wireless networks, offering great potential for the revolution of cyber-physical systems [1], [2], [3], [4]. In the cyber-physical system, sensing information is wirelessly transmitted from sensors to the control center, which performs complex computations and then delivers control commands to actuators for operating control systems [5]. It can be seen that the bidirectional wireless transmissions of sensing and action information are crucial for ensuring the stability of control systems. In general, the more state and control information is delivered, the better the estimation and control performance will be [6]. While recent advancements have alleviated traditional spectrum scarcity issues, the fundamental challenges in closing all control loops persist due to the stochastic nature of wireless communications. Time-varying channel conditions (e.g., fading and interference) induce uncertain communication delays and packet loss rates, which can disrupt the synchronicity required for closed-loop control [7], [8]. Furthermore, the contention for shared communication resources among multiple control systems often leads to non-deterministic scheduling patterns, potentially causing critical control signals to miss their deadlines [9]. These communication-induced uncertainties may propagate through feedback loops, resulting in performance degradation and even system instability.

Significant progress has been made on designing estimation/control methods to mitigate the effects of imperfect wireless transmission on control systems [10]. Qiao et al. [11] proposed an energy-aware sensor scheduling and opportunistic transmission scheme to balance the estimation performance and resource consumption. Chang et al. [12] investigated sensor scheduling for state estimation of heterogeneous systems over constrained and lossy wireless channels, which achieved a near-optimal estimation performance with reduced computation time. Zhang et al. [13] proposed an event-triggered finite-time distributed estimation algorithm to precisely estimate the state of the nonlinear system with maneuvering targets. Yu et al. [14] presented

a novel fault-tolerant control algorithm to guarantee all signals were bounded in spite of the occurrence of multiple actuators and sensors faults. Wen et al. [15] proposed a co-design architecture of sampling-scheduling-control to improve the overall system performance, including control cost and network energy consumption. Wang et al. [16] proposed a state-estimation-based control algorithm in a backward recursion manner to regulate vehicle's motion. While these studies mainly treat wireless communication networks as unpredictable and uncontrollable variables, ignoring the potential adaptability of wireless networks, which results in inefficient and overly conservative.

As the communication system is one of the two fundamental components in cyber-physical systems, communication optimization is crucial for system-level performance enhancement [17], [18], [19]. Zhang et al. [20] investigated the joint uplink and downlink robust transmission design for cell-free networks. Lee et al. [21] investigated reconfigurable intelligent surface-aided frequency division duplexing communication systems to support the simultaneous transmissions for the downlink and uplink signals. Zeng et al. [22] investigate unmanned aerial vehicle assisted communication systems that require quasi-balanced data rates in uplink and downlink. These works mainly devote to improve the transmission rate or energy efficiency, making it challenging to directly apply them into the full-loop control of cyber-physical systems.

In this paper, we design an uplink-downlink transmission scheme for the full-loop control under the limitation of radio resources. In the uplink transmission, the simultaneous transmission of sensing information from multiple sensors to the remote center is a many-to-one transmission process, then the OFDMA technology is used to mitigate the interference among sensors. In the downlink transmission, the concurrent transmission of small-packet control information from the controller to multiple actuators is a one-to-many transmission process, then the multicast technology is used to used to balance the transmission latency and resource efficiency. The contributions of this paper are summarized as follows.

- We analyze the impact of uplink sensing information and downlink control information transmission on the full-loop control performance, which makes it possible to achieve the integrated design of communication and control to enhance the overall performance.
- The proposed multicast-based downlink transmission scheme could significantly reduce the head overhead of small packets by aggregating multiple actuators into one multicast group, and then balance network resource utilization and control performance.
- The uplink-downlink transmission and the full-loop control are integratedly designed to achieve the control accuracy enhancement and the control-communication cost reduction with the limited radio resource.

The remainder of this paper is organized as follows. The system model and problem formulation is presented in Section III. In Section IV, integrated design scheme of uplink-downlink transmission and control is proposed to minimize the overall cost. Simulation results and main conclusions are shown in Sections V and VI, respectively.

II. Related Works

A. Estimation and Control Design for Cyber-Physical Systems

For cyber-physical systems constrained by communication resources, some existing works focus on how to design advanced estimation and control methods to mitigate the impact of communication on control performance. From the perspective of state estimation, Zhang et al. [23] studied the distributed secure state estimation problem for cyber-physical systems subjected to false data injection attacks. Moreover, a novel distributed framework was proposed for remote state estimation based on distributed Kalman filtering technology, where the sensors gather neighboring measurement information and then sent it and local estimation to remote estimators through wireless channels. Chen et al. [24] considered the situation where the transmitted binary bits may be flipped over noisy communication channels, and designed a distributed resilient estimation scheme under a bit-flipped detection mechanism to achieve a reliable estimation of the cyber-physical systems. Yang et al. [25] proposed a Kullback-Leibler divergence based detector against stochastic linear attacks for distributed state estimation over wireless sensor networks, which combines the Mahalanobis distance as well as the Burg matrix divergence between covariance. Xin et al. [26] presented the innovative virtual sensor based secure state estimator framework, which utilizes Virtual SensorNet to generate preliminary estimations when a major sensor is compromised and integrates deep reinforcement learning to refine these estimations online. From the perspective of control design, He et al. [27] proposed a novel event-triggered MPC framework for perturbed nonlinear cyber–physical systems with input and state constraints to reduce the communication and computational resource consumption while ensuring the control performance. H. Mamduhi et al. [28] described a novel cross-layer interactive ecosystem for real-time cyber-physical systems wherein heterogeneous physical systems ware aware of the diverse network services while their time sensitivity requirements ware shared with the network for an efficient service allocation. Lucia et al. [29] developed a novel control architecture for constrained networked control systems to mitigate the undesired effects arising when stealthy attacks affect the nominal behavior of constrained cyber-physical systems. Ren et al. [30] investigated the group formation control problem for cyber-physical systems with random communication constraints, and proposed a data-driven predictive control strategy to actively compensate for communication constraints and achieve group formation. Fu et al. [31] employed decentralized event-triggering mechanisms for wireless cyber–physical systems whose sensors are distributed and bandwidths are limited, which can largely reduce the transmissions with the help of additional dynamic variables. Ji et al. [32] proposed a observability guaranteed method based on the detailed analysis of the relationship between edge sensing, observability condition, and control performance, which could achieve the lower sensing cost and better control performance with the sensing and control co-design. Ren et al. [33] studied the distributed group coordinated control problem of cyber-physical systems with multi-agent architecture, and proposed a data-driven cloud edge predicted control scheme to ensure

that the agents can effectively achieve coordination while also overcoming communication constraints. Moreover, some other works investigates the secure control problem due to the attack introduced by networks. Ma et al. [34] developed a security control framework to codesign the switched controller and event-triggered mechanism, with which the closed-loop system can achieve a better control performance than traditional dynamic event-triggered mechanisms in the transient process. Liu et al. [35] proposed a novel secure control method based on the dynamic-memory event-triggered scheme for discrete-time cyber-physical power systems, which has not only enhanced the system's secure capabilities, but also effectively lowered the demand for communication bandwidth, thereby improving the security and sustainability, especially in hard-to-reach areas where the self-sustainable sensors and controllers are deployed. Zhao et al. [36] presented a secure control strategy under fast time-varying actuator attacks for cyber-physical systems, and the L_2 gain secure controller was designed to guarantee the stability. Zhang et al. [37] investigated the observer-based control problem for the cyber-physical systems model with dual-scale attacks. Since the slow and fast transmission channels have different time scales, a dual-rate sampling strategy has been designed, and the modeling of dual-scale attacks has been implemented. Guan et al. [38] investigated the slidingmode fault-tolerant secure control issue for cyber-physical systems under both cyber jamming attacks and multiple physical intermittent faults. Moreover, a Stackelberg game model is adopted to depict the complex interaction between the transmitter and the attacker to counter the attack strategy of the intelligent attacker. Ma et al. [39] designed a novel state observer that can be driven by actuator faults and intermittent available signals arising from triggered attack-state signals, which can realize directly triggering the states after deception attacks and avoid the problem of virtual controller non-dierentiability under the backstepping framework. Gao et al. [40] investigated the event-triggered adaptive fixed-time secure control problem for nonlinear cyber-physical systems under false data-injection attacks, and developed a dynamic switching mechanism based on the fixed-time stability theorem.

B. Communication Design for Cyber-Physical Systems

For cyber-physical systems, the bidirectional wireless transmissions of sensing and action information are crucial for ensuring the stability of control systems [41]. Some existing works focus on how to provide the satisfying information exchanging service for closed-loop control over wireless networks. Pang et al. [42] proposes a practical communication-control model for wireless networked control systems, which captures correlated dynamics among spatially distributed sensors and actuators sharing limited wireless resources over multi-state Markov blockfading channels. Moreover, a deep reinforcement learning algorithm is developed to scale efficiently by managing hybrid action spaces, capturing communication-control dependencies, and maintaining robust performance under time-correlated dynamics and resource constraints. Huang et al. [43] designed a core-agnostic and cost-effective solution named Hirail to achieve the smooth evolution of long-distance deterministic networks, which could meet the bounded delay and jitter demands, and have advantages on the performance and overhead. Lyu et al. [44] proposed an automated guided vehicle assisted adaptive cooperative transmission scheme to minimize the mean square error of state estimation at a low energy cost. Moreover, a novel performance index, estimation gain, is introduced to evaluate the benefit of scheduling one sensor for estimation error reduction. Yan et al. [45] investigated the joint beamforming design in a multi-functional reconfigurable intelligence surface-aided uplink communication system, which could amplify incident signals from both sides without signal leakage by using the mode switching protocol. Huang et al. [46] proposed a learning-based robust resource allocation considering overlapping interference and age-of-information sensitive services requirements for the ultradense industrial internet of Things networks with overlapping interference. Lyu et al. [47] derived a closed-form expressing of estimation error with respect to offloading delay to indicate that adjusting offload delay on demand is necessary for estimation error reduction. Based on the finding, an adaptive edge sensing scheme is designed to minimize estimation error by jointly optimizing task offloading and sensor scheduling. Xie et al. [48] developed a dynamic scheduling scheme that prioritizes computing tasks and matches tasks to computing resources in real time, and proposed an improved deep reinforcement learning algorithm to improve task success rates and minimize execution delays. Ernest and Madhukumar [49] separatively derived new closed-form expressions for the violation probability of peak age of information and the mean peak age of information for the offloading strategy design with awareness of the uplink timeliness, joint uplink-and-computing timeliness, and cloud-only computation. Zhang et al. [50] proposed an urgency-based fast flow scheduling algorithm to address the issue, that leverages domainspecific optimizing strategies with a focus on traffic delay urgency inspired by greedy algorithm for priority allocation across hops and flows, complemented by preprocessing for scenario solvability and dynamic verification to ensure scheduling feasibility. Wen et al. [51] proposed a contract theory model and developed a sustainable diffusion-based soft actor-critic algorithm to identify the optimal feasible contract, which could enable efficient digital twins construction and monitor Industrial cyber-physical systems. Lyu et al. [52] presented a transmission-estimation co-design framework to lay down the foundation for guaranteeing the prescribed estimation accuracy with limited communication resources. Moreover, a hierarchical transmission-estimation approach was proposed to improve the transmission reliability and estimation accuracy according to system dynamics. Chen et al. [53] designed a hierarchical algorithm to focus on the distributed guaranteed-performance consensus problem of multi-agent systems subjected to communication faults. Moreover, the sufficient conditions for the boundedness of all signals in the closed-loop system are derived based on Lyapunov theory. Zhang et al. [23] proposed a novel distributed framework for remote state estimation based on distributed Kalman filtering technology, where the sensors gather neighboring measurement information and send it and local estimation to remote estimators through wireless channels.

Liu et al. [35] proposed a novel secure control method for discrete-time cyber-physical power systems to guarantee the exponential stability with limited communication resources for data transmission. From the perspective of cost reduction and resource limitation, Cai et al. [2] proposed a novel mechanism for data uploading in smart cyber-physical systems, which considers both energy conservation and privacy preservation. This mechanism preserves privacy by concealing abnormal behaviors of participants, while still achieves an energy-efficient scheme for data uploading by introducing an acceptable number of extra contents. Nagarajan et al. [54] proposed IoT-based healthcare cyber-physical system that provided effective resource utilization at fog and cloud levels with minimum execution cost. Afrin et al. [3] developed a congestion game-theoretic robotic edge resource allocation mechanism for cyber-physical social system, which not only maintains the quality-of-service by meeting task completion deadlines but also satisfies the energy constraints of resources. Cui et al. [55] proposed an intelligent optimization technology framework based on data processing to deal with the problem of redundant attributes of massive and high-dimensional data in the cyber-physical social system. Chen et al. [56] proposed a collaborative filtering service recommendation algorithm that combines heterogeneous information networks and topic models for the cyber-physical social system. Mughal et al. [57] presented a new resource allocation scheme that used multiple wireless communication technologies and link lifetimes simultaneously during the decision-making process to meet the requirements of resource-intensive mobile cyber-physical social systems applications. Chen et al. [58] studied the dynamic of cascading failure iterating between physical power grid and communication network, and further proposed the attack strategy to locate the critical nodes which can seriously damage the cyber-physical power systems. Dong et al. [59] proposed a heterogeneous cyber-physical system model with weak dependency, in which the two networks overlap geographically and have heterogeneous models. Qin et al. [60] proposed an remote terminal unit satellite-terrestrial multi-hop network with energy cooperation for remote cyber-physical power systems, and introduced a multi-agent deep reinforcement learning approach to efficiently solve the formulated problem. Peng et al. [61] proposed a more general attack model which is not subject to any constraints, and designed a dynamics controller whose internal state is transmitted in real-time from the communication layer to the physical layer through the information exchange with neighboring subsystems. Li et al. [62] built an air-ground nonlinear swarm system with aggregation-dispersion properties, and proposed a fog-cloud cooperative control method to ensure the secure consistency of the swarm under denial of service attacks.

C. Uplink and Downlink Transmission Design

As the communication system is one of the two fundamental components in cyber-physical systems, communication optimization is crucial for system-level performance enhancement [63], [64]. In the uplink transmission, Katwe et al. [65] investigated an intelligent reflecting surface aided uplink rate-splitting multiple access system and got higher achievable sum-rate throughput. Xu et al. [66] proposed an aggregated transmit power minimization problem constrained by the delay bound. Li et al. [67] investigated a cell-free massive multiple-input-multiple-output system and designed an iterative search-based two-stage energy efficiency optimization algorithm for the uplink communication. The designed algorithm could reduce the demand for training samples and training time overhead by employing deep transfer learning to adjust parameters of the convolutional neural network architecture to accommodate the potential of dynamic communication scenarios. In the downlink transmission, Jiao et al. [68] proposed a delay-efficient energy-aware broadcast scheduling algorithm to adapt to wireless powered Internet of Things. Zhang et al. [69] proposed a proactive orthogonal frequency division multiple access downlink system framework, and designed a reinforcement learning-based online model-free algorithm to ensure transmission reliability while providing rapid radio resource allocation. Lyu et al. [70] proposed a beamforming-assisted hierarchical coordinated transmission strategy based on channel conditions and system dynamics to alleviate the impact of unreliable transmission on the control performance.

Recently, some works focus on the joint design of uplink and downlink transmissions. Yu et al. [71] studied a joint uplink and downlink resource allocation algorithm to distribute radio resources in each control period among machines to increase resource utilization. F. Kimaryo et al. [72] analyzes the achievable uplink and downlink capacity where both the base station and the user are equipped with dynamic metasurface antennas. Li et al.. [73] proposed an energy-efficient packet delivery mechanism incorparated with frequency-hopping and proactive dropping, which could reduce the average total power under the transmission requirements by jointly optimizing bandwidth allocation and power control of uplink and downlink, antenna configuration, and subchannel assignment. Zhang et al. [74] investigated the joint uplink and downlink resource allocation in a multiuser multiple-input single-output orthogonal frequency-division multiple access system in a finite blocklength regime, and proposed a deep reinforcement learning based proximal policy optimization algorithm with a modified architecture to solve the sequential decision making problem. Chen et al. [75] proposed a novel downlink and uplink cooperative scheme for the joint communication and sensing system, including a unified multiple signal classification based joint communication and sensing scheme and a downlink and uplink cooperative fusion method. Guo et al. [76] employed the non-orthogonal multiple access technology in both uplink and downlink relaying hops in an amplify-and-forward based relaying network with multiple source-destination user pairs, and proposed a novel recursive two-hop grouping algorithm to efficiently group users and increase the system sum rate. Chen et al. [77] proposed a concurrent downlink and uplink scheme for the joint communication and sensing system, where the base station can use the echo of transmitted dedicated signals for sensing in the uplink timeslot, while performing reliable uplink communication. Moreover, a novel successive interference cancellation-based processing method was proposed to enable the estimation of

TABLE I
SUMMARY OF STUDIES ON UPLINK-DOWNLINK TRANSMISSION FOR NETWORKED CONTROL SYSTEMS

References	Communication Design			Control Performance
	Uplink	Downlink	Up-Down	
Ref. [45] Ref. [48] Ref. [49]	✓	×	×	×
Ref. [42] Ref. [44] Ref. [47]	✓	×	×	✓
Ref. [72] Ref. [73]	×	✓	×	×
Ref. [74]	×	✓	×	✓
Ref. [75] Ref. [76] Ref. [77] Ref. [78] Ref. [78] Ref. [79] Ref. [80] Ref. [81]	×	×	✓	×
This Work	×	×	✓	✓

uplink communication symbols and downlink sensing parameters. Zhou et al. [78] proposed a transmission scheme for fog computing-enabled internet of medical things to minimize the offloading and feedback duration, where the uplink and downlink rate splitting technology is utilized to offer flexible co-channel interference management. Xia et al. [79] considered the problem of jointly optimizing duplex mode selection and secrecy transceivers to maximize the overall secrecy spectral efficiency, where the information signals at access points are injected with artificial noise to prevent interception of information by eavesdroppers. Moreover, a two-loop strategy is proposed to deal with the complex optimization problem, since the downlink secure beamforming, uplink transmission power, and uplink receivers are tightly coupled in both the objective function and the constraints. A summary the above discussion is provided in Table I.

III. SYSTEM MODEL AND PROBLEM FORMULATION

In cyber-physical systems, sensors, controllers, and actuators are connected via wireless networks. In particular, sensors are tasked with monitoring key system parameters, such as temperature and humidity. The acquired sensory data is subsequently transmitted via the uplink to an access point (AP), where the controller processes data to estimate the system state and generate appropriate control commands. These commands are then transmitted through downlink to the actuators for executing the necessary actions to maintain the stable operation. Since control commands typically consist of small data payloads, conventional unicast transmission schemes often incur inefficient resource utilization due to low payload-to-overhead ratios. This inefficiency makes unicast transmission cost-ineffective for control applications, particularly in resource-constrained systems. To address this issue, multiple shortlength control data-packets are integrated into a long-length data-packet, and then the integrated data-packet is broadcasted to a group of actuators on the same wireless channels. As the broadcasting performance is limited

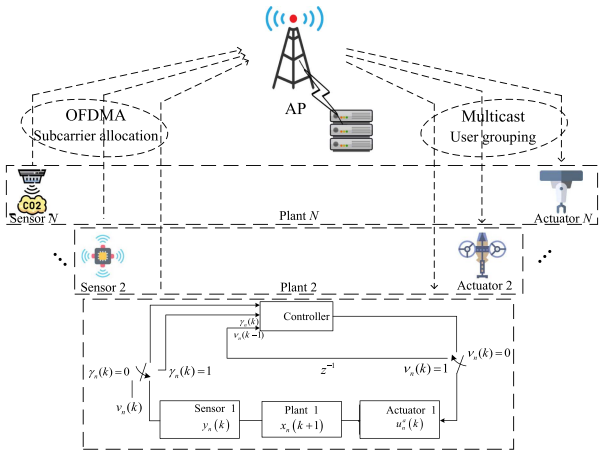

Fig. 1. Transmission architecture for cyber-physical systems.

by the one with worst channel condition, it is necessary to well determine the broadcasting group based on wireless channel conditions. To this end, the multicasting technology is used, which makes it possible to flexibly determine how many and which data packets of control commands to be integrated together. In the downlink transmission, the concurrent transmission of small-packet control information from the controller to multiple actuators is a one-to-many transmission process, the proposed multicast-based downlink transmission scheme could significantly reduce the head overhead of small packets by aggregating multiple actuators into one multicast group, and then balance network resource utilization and control performance.

A. Control System Model

The control system comprises N control loops, each consisting of a sensor-actuator pair, as shown in Fig. 1. The considered linear stochastic system with intermittent observations and control input is described as:

$$x_n(k+1) = A_n x_n(k) + D_n u_n^{\mathrm{a}}(k) + w_n(k), \tag{1}$$

$$u_n^{\mathrm{a}}(k) = \nu_n(k) u_n^{\mathrm{c}}(k), \tag{2}$$

$$y_n(k) = \gamma_n(k) C_n x_n(k) + z_n(k), \forall n \in \mathcal{N}, \tag{3}$$

where $x_n(k) \in \mathbb{R}^{a_x}$ is the system state at control step k, $u_n^{\mathrm{a}}(k) \in \mathbb{R}^{a_u}$ is the control input received by the actuator n, $u_n^{\mathrm{c}}(k)$ is the desired control input computed by the controller, and $y_n(k) \in \mathbb{R}^{a_y}$ is the measurement from sensor n. The matrices $A_n \in \mathbb{R}^{a_x \times a_x}$, $D_n \in \mathbb{R}^{a_x \times a_u}$ and $C_n \in \mathbb{R}^{a_y \times a_x}$ are the state transition, input and measurement matrices of sensor n, respectively. $(x_n(0), w_n(k), z_n(k))$ are Gaussian, uncorrelated, and white, with means $(\bar{x}_n(0), 0, 0)$ and covariances $(\Sigma_n(0), Q_w, Q_z)$ [80]. $\gamma_n(k)$ denotes whether the sensing information is received by the controller. If data packet of sensing information is successfully received, $\gamma_n(k) = 1$, i.e., $y_n(k) = C_n x_n(k) + z_n(k)$. Otherwise, $\gamma_n(k) = 0$, i.e., $y_n(k) = z_n(k)$. $\nu_n(k)$ denotes whether the control information is received by the actuator n. If data packet of control information is successfully received, $\nu_n(k) = 1$, i.e., $u_n^{\mathrm{a}}(k) = u_n^{\mathrm{c}}(k)$. Otherwise, $\nu_n(k) = 0$, i.e., $u_n^{\mathrm{a}}(k) = \mathbf{0}$.

Equations for optimal estimator are derived using arguments similar to those used in standard Kalman filtering [81]. Then, the sensing error caused by the packet loss of sensory data could be expressed as

$$\begin{aligned} e_n^{\mathrm{s}}(k) &= x_n(k) - \hat{x}_n(k|k) \\ &= (I - \gamma_n(k) G_n(k) C_n)\, e_n(k|k-1) - \gamma_n(k) G_n(k) z_n(k), \end{aligned} \tag{4}$$

where I is the unit matrix, $G_n(k)$ is the Kalman gain, $\hat{x}_n(k|k)$ is the system state estimation, and the prior estimation error $e_n(k|k-1)$ is the one-step prediction value for step k.

According to optimal control theory [82], the optimal control input is given by

$$\begin{aligned} u_n^{\mathrm{c}}(k) = &-\left(D_n' W_n(k+1) D_n + U_n(k)\right)^{-1} \\ &D_n' W_n(k+1) A_n \hat{x}_n(k|k) = L_n(k) \hat{x}_n(k|k), \end{aligned} \tag{5}$$

where the matrix $W_n(k)$ could be obtained with the iterative computation manner. $U_n(k)$ is the positive definite weight. In this case, the control error caused by the packet loss of control command is expressed as

$$e_n^{\mathrm{c}}(k) = u_n^{\mathrm{c}}(k) - u_n^{\mathrm{a}}(k) = (1 - \nu_n(k))\, L_n(k) \hat{x}_n(k|k). \tag{6}$$

It can be seen that if control information is delayed or lost, the actuator will be unable to receive the already computed control decision, which can significantly increase the control error. Furthermore, this scenario also consumes uplink network resources without contributing to any improvement in control accuracy. This is because the successfully received sensing information remains unused by the actuator, meaning that the control system fails to benefit from the sensing data transmitted over the wireless network. On the other hand, the impact of delayed or lost control information differs from that of sensing information. This is because the controller can perform state estimation to compensate for the loss of sensing information, thereby mitigating the effect of its delay or loss on the control error. In contrast, the actuator merely executes the received control commands without any ability to compensate for missing information. As a result, the delay or loss of control information has a more substantial impact on the control error.

B. Communication Network Model

The spectral resources of the same bandwidth are shared by the uplink and downlink transmissions through the adoption of time-division multiplexing technology. The sensor-actuator pairs are denoted by $\mathcal{N} = \{1, 2, \ldots, N\}$, where the association between sensors and actuators is pre-established.

In the uplink transmission, OFDMA is considered due to its advantage on connectivity and spectrum utilization [83]. The mutually orthogonal subcarriers are denoted by $\mathcal{S} = \{1, 2, \ldots, S\}$. The total bandwidth B is evenly distributed into each subcarrier, i.e., the bandwidth of each subcarrier is $\bar{b} = B/S$. Let $\theta_{n,s}(k) = 1$ denote that subcarrier s is assigned to sensor n at control step k. Otherwise, $\theta_{n,s}(k) = 0$. Then, the signal-to-noise ratio (SNR) of sensor n on subcarrier s at control step k is given by

$$\Gamma_{n,s}(k) = \frac{p_n(k) h_{n,s}(k)}{\sigma^2}, \forall n \in \mathcal{N}, \forall s \in \mathcal{S}, \tag{7}$$

where $p_n(k)$ is the transmit power of sensor n, $h_{n,s}(k)$ is the power gain of sensor n on subcarrier s, and σ^2 is the noise power [84]. The achievable transmission rate of sensor n on subcarrier s can be expressed as

$$r_{n,s}(k) = \theta_{n,s}(k) \bar{b} \log_2\left(1 + \Gamma_{n,s}(k)\right), \forall n \in \mathcal{N}, \forall s \in \mathcal{S}. \tag{8}$$

Then, the uplink transmission delay from sensor n to AP is given by

$$\bar{t}_n(k) = \frac{\bar{d}_n(k)}{r_{n,s}(k)}, \forall s \in \mathcal{S}, \tag{9}$$

where $\bar{d}_n(k)$ is the sensory data size of sensor n.

In the downlink transmission, the concurrent transmission of small-packet control information from the controller to multiple actuators is a one-to-many transmission process, then the multicast technology is used to balance the transmission latency and resource efficiency [85]. In this case, N actuators are divided into M groups, denoted by $\mathcal{M} = \{1, 2, \ldots, M\}$. Let $\varphi_{n,m}(k) = 1$ denote actuator n is allocated to multicast group m at control step k. Otherwise, $\varphi_{n,m}(k) = 0$. The set of actuators assigned to group m is denoted as $\mathcal{N}_m$. The SNR of the received signal by actuator n in group m is expressed as

$$\Gamma_{n,m}(k) = \frac{h_n(k) q_m(k)}{\sigma^2}, \forall n \in \mathcal{N}, \forall m \in \mathcal{M}, \tag{10}$$

where $h_n(k)$ is the power gain of actuator n, and $q_m(k)$ is the transmit power assigned to group m by AP. The achievable transmission rate of multicast group m is

$$r_m(k) = \underline{b}_m(k) \log_2\left(1 + \min_{n \in \mathcal{N}_m} \Gamma_{n,m}(k)\right), \forall m \in \mathcal{M}, \tag{11}$$

where $\underline{b}_m(k)$ is the transmission bandwidth for multicast group m. The transmission delay of group m can be expressed as $t_m(k) = \frac{\sum_{n \in \mathcal{N}_m} \underline{d}_n(k)}{r_m(k)}$, where $\underline{d}_n(k)$ is the size of data packet needed to be received by actuator n. The transmission rate of actuator n in group m is

$$r_{n,m}(k) = \underline{b}_m(k) \log_2\left(1 + \Gamma_{n,m}(k)\right), \forall n \in \mathcal{N}, \forall m \in \mathcal{M}. \tag{12}$$

The achievable transmission rate from AP to actuator n is

$$r_n(k) = \sum_{m \in \mathcal{M}} \varphi_{n,m}(k) r_{n,m}(k), \forall n \in \mathcal{N}. \tag{13}$$

Therefore, the downlink transmission delay from AP to actuator n is given by

$$\underline{t}_{n,m}(k) = \frac{\sum\limits_{n \in \mathcal{N}_m} \underline{d}_n(k)}{r_n(k)} = \frac{\sum\limits_{n \in \mathcal{N}} \varphi_{n,m}(k) \underline{d}_n(k)}{r_n(k)}, \forall n \in \mathcal{N}. \tag{14}$$

Assume that there are K control steps denoted by $\mathcal{K} = \{1, 2, \ldots, K\}$, each with a duration of T. The division point of uplink and downlink transmission is denoted as $\eta(k)$, i.e., $T_{\mathrm{s}}(k) = \eta(k)T$ and $T_{\mathrm{a}}(k) = (1 - \eta(k))T$. To be specific, if

uplink sensing information is successfully received by the controller at control step k, it means that $\bar{t}_n(k) \leq T_{\rm s}(k)$ and $\gamma_n(k) = 1$. Otherwise, $\gamma_n(k) = 0$. Similarly, if downlink control information is successfully received by the actuator at control step k, it means that $\underline{t}_{n,m}(k) \leq T_{\rm a}(k)$ and $\nu_n(k) = 1$. Otherwise, $\nu_n(k) = 0$. Therefore, the overall control performance at each step depends heavily on the transmission timelessness of both uplink sensing information and downlink control information, since the transmission failures of sensing or control information will negatively impact the effectiveness of the closed-loop control system.

C. Problem Formulation

The overall cost composed of control cost and communication cost is used to evaluate the system performance. In order to minimize the overall cost, we integratedly design the division of uplink/downlink transmission duration, subcarrier allocation and transmit power in uplink, multicast grouping and bandwidth allocation in downlink. The constrained overall cost minimization problem is formulated as

$$\mathcal{P}_0: \min_{\boldsymbol{\theta},\boldsymbol{p},M,\boldsymbol{\varphi},\underline{\boldsymbol{b}},\boldsymbol{q},\eta} \frac{1}{K}\sum_{k\in\mathcal{K}}\left[J(k)+\beta E(k)\right] \tag{15}$$

$$\text{s.t.} \sum_{n\in\mathcal{N}} \theta_{n,s}(k) = 1,\ \forall s \in \mathcal{S}, \tag{15a}$$

$$\sum_{s\in\mathcal{S}} \theta_{n,s}(k) = 1,\ \forall n \in \mathcal{N}, \tag{15b}$$

$$0 \leq p_n(k) \leq p_{\max},\ \forall n \in \mathcal{N}, \tag{15c}$$

$$\sum_{m\in\mathcal{M}} \underline{b}_m(k) \leq B, \tag{15d}$$

$$\sum_{m\in\mathcal{M}} q_m(k) \leq q_{\max}, \tag{15e}$$

$$\sum_{m\in\mathcal{M}} \varphi_{n,m}(k) = 1,\ \forall n \in \mathcal{N}, \tag{15f}$$

$$\mathcal{M} = \{1, 2, \ldots, M\},\ 1 < M \leq N, \tag{15g}$$

$$\theta_{n,s}(k) \in \{0,1\},\ \forall n \in \mathcal{N}, \forall s \in \mathcal{S}, \tag{15h}$$

$$\varphi_{n,m}(k) \in \{0,1\},\ \forall n \in \mathcal{N}, \forall m \in \mathcal{M}, \tag{15i}$$

$$\eta(k) \in \left(0,1\right), \tag{15j}$$

where β is a preference factor, $J(k) = sum_{n\in\mathcal{N}}\{\mathbb{E}[e_n^{\rm s}(k)^{\rm T}e_n^{\rm s}(k)] + \mathbb{E}[e_n^{\rm c}(k)^{\rm T}e_n^{\rm c}(k)]\}$. $E(k)$ is equal to the sum of $E_1(k)$ and $E_2(k)$, where $E_1(k) = \sum_{n\in\mathcal{N}}\gamma_n(k)p_n(k)\bar{t}_n(k)$ and $E_2(k) = \sum_{m\in\mathcal{M}} q_m(k)\frac{\sum_{n\in\mathcal{N}_m} d_n(k)}{r_m(k)}$. $p_{\max}$ and $q_{\max}$ are the maximum transmit power of the sensor and the AP, respectively. Constraints (15a) and (15b) indicate the one-to-one matching relationship between the sensor and the subcarrier. Constraints (15c)–(15e) are bandwidth and power constraints. Constraint (15f) restricts each actuator to be assigned to only one multicast group. Constraints (15g)–(15h) describe the feasible regions of optimal variables. Moreover, the variable $\boldsymbol{\theta}$ denotes the matching relationship between channels and sensors in the uplink transmission process. The element $\theta_{n,s}(k)$ denotes whether the n-th channel is matched to the s-th sensor at control step k. If so, $\theta_{n,s}(k) = 1$. Otherwise, $\theta_{n,s}(k) = 0$. $\boldsymbol{p}$ denotes the transmit power of sensors, and $p_n(k)$ denotes the transmit power of the n-th sensor at control step k. $\boldsymbol{\varphi}$ denotes the grouping situation of actuators, and $\varphi_{n,m}(k)$ denotes whether the n-th actuator is allocated to multicast group m at control step k. If so, $\varphi_{n,m}(k) = 1$. Otherwise, $\varphi_{n,m}(k) = 0$. $\underline{\boldsymbol{b}}$ denotes the bandwidth allocation in the downlink transmission process, and $\underline{b}_m(k)$ denotes the transmission bandwidth for multicast group m at control step k. $\boldsymbol{q}$ denotes the transmit power of AP in the downlink transmission process, and $q_m(k)$ denotes the transmit power assigned to group m by AP at control step k.

IV. Joint Uplink-Downlink Transmission Design and Control

The original problem $\mathcal{P}_0$ is a mixed-integer nonlinear programming (MINLP) problem, since it includes a nonlinear objective function with the time-accumulated term of the overall cost, as well as, mixed-integer variables (binary variables $\boldsymbol{\theta}$ and $\boldsymbol{\varphi}$, continuous variables $\boldsymbol{p}$, $\underline{\boldsymbol{b}}$, $\boldsymbol{q}$ and η), which is challenging to be directly solved. For the convenience of solving, we focus on one step problem. Therefore, the overall optimization problem can be split into multiple subproblems at different control steps. In this way, the original problem is decomposed into K problems according to control steps, with each one aiming at minimizing the instantaneous overall cost, i.e., $J(k) + \beta E(k)$.

For each control step, the value of uplink/downlink transmission duration division point $\eta(k)$ determines the tolerable delay for uplink transmission $T_{\rm s}(k)$ and downlink transmission $T_{\rm a}(k)$, which in turn rely heavily on the transmission statuses of sensory data and control commands, i.e., $\gamma_n(k)$ and $\nu_n(k)$. When $\eta(k)$ is given, the constraints of the original problem can be divided into two parts. Then, the problem at each control step can be further decomposed into two sequential subproblems, namely, the uplink transmission subproblem and the downlink transmission subproblem. The uplink transmission subproblem at control step k is expressed as

$$\mathcal{SP}_1: \min_{\boldsymbol{\theta},\boldsymbol{p}} \sum_{n\in\mathcal{N}} \mathbb{E}\left[e_n^{\rm s}(k)^{\rm T}e_n^{\rm s}(k)\right] + \beta_1 E_1(k)$$
$$\text{s.t.}\quad \text{(15a)}, \text{(15b)}, \text{(15c)}, \text{(15h)}, \tag{16}$$

where β_1 is a preference factor. When obtaining the subcarrier allocation and sensor transmit power, the transmission status of uplink sensory data can be determined, and then the controller proceeds to perform state estimation and calculate control commands based on the received data.

Subsequently, the control commands are transmitted to the actuators. The downlink transmission subproblem includes multicast group partitioning, bandwidth allocation, and power allocation, which is expressed as

$$\mathcal{SP}_2: \min_{M,\boldsymbol{\varphi},\underline{\boldsymbol{b}},\boldsymbol{q}} \sum_{n\in\mathcal{N}} \mathbb{E}\left[e_n^{\rm c}(k)^{\rm T}e_n^{\rm c}(k)\right] + \beta_2 E_2(k)$$
$$\text{s.t.}\quad \text{(15d)}, \text{(15e)}, \text{(15f)}, \text{(15g)}, \text{(15i)}, \tag{17}$$

where β_2 is a preference factor. Moreover, $\beta = \beta_1 + \beta_2$. For the remainder of this section, an alternating resource optimization algorithm is proposed to solve $\mathcal{SP}_1$, and a multicast resource allocation algorithm is utilized to solve $\mathcal{SP}_2$.

A. Uplink Transmission Optimization for Sensing Information

The uplink transmission subproblem $\mathcal{SP}_1$ is still non-convex due to the nonlinear objective function and the non-convex constraints. In order to solve the problem efficiently, the objective function is firstly transformed and simplified. According to (4), the mean square error of state estimation is calculated as

$$\mathbb{E}\left[e_n^s(k)^{\mathrm{T}} e_n^s(k)\right] = c_n^1(k) - c_n^2(k)\mathbb{E}\left[\gamma_n(k)\right], \tag{18}$$

where

$$\begin{aligned}
c_n^1(k) &= c_n^3(k)^{\mathrm{T}} c_n^3(k) + c_n^4(k)^{\mathrm{T}} c_n^3(k) \\
&\quad + c_n^3(k)^{\mathrm{T}} c_n^4(k) + c_n^4(k)^{\mathrm{T}} c_n^4(k), \\
c_n^2(k) &= c_n^3(k)^{\mathrm{T}} c_n^3(k) + c_n^4(k)^{\mathrm{T}} c_n^3(k) + c_n^3(k)^{\mathrm{T}} c_n^4(k), \\
c_n^3(k) &= G_n(k) C_n e_n\left(k|k-1\right) + G_n(k) z_n(k), \\
c_n^4(k) &= e_n(k|k-1) - G_n(k) C_n e_n(k|k-1) - G_n(k) z_n(k).
\end{aligned}$$

In (18), $\mathbb{E}[\gamma_n(k)]$ is the probability of successful transmission for the sensory data of sensor n, which is elaborated as

$$\begin{aligned}
\mathbb{E}\left[\gamma_n(k)\right] &= \Pr\left\{\bar{b}\log_2\left(1 + \frac{p_n(k) h_{n,s}(k)}{\sigma^2}\right) \geq \frac{\bar{d}_n(k)}{T_{\mathrm{s}}(k)}\right\} \\
&= \Pr\left\{h_{n,s}(k) \geq \frac{\sigma^2\left[2^{\frac{\bar{d}_n(k)}{T_{\mathrm{s}}(k)\bar{b}}} - 1\right]}{p_n(k)}\right\}, \forall s \in \mathcal{S}.
\end{aligned} \tag{19}$$

Since the channel gain follows the Rayleigh distribution, the cumulative distribution function is $F(x;\sigma) = 1 - e^{\frac{-x^2}{2\sigma^2}}$. Then, $\mathbb{E}[\gamma_n(k)]$ can be further expressed as

$$\mathbb{E}\left[\gamma_n(k)\right] = e^{-\frac{\sigma^2\left[2^{\frac{\bar{d}_n(k)}{T_{\mathrm{s}}(k)\bar{b}}} - 1\right]}{2p_n(k)}}, \forall n \in \mathcal{N}. \tag{20}$$

Therefore, problem $\mathcal{SP}_1$ could be rewritten as

$$\begin{aligned}
&\min_{\boldsymbol{\theta},\boldsymbol{p}} \sum_{n\in\mathcal{N}} \left\{c_n^1(k) - c_n^2(k)\mathbb{E}\left[\gamma_n(k)\right]\right\} + \beta_1 E_1(k) \\
&\text{s.t.} \quad \text{(15a)}, \text{(15b)}, \text{(15c)}, \text{(15h)}.
\end{aligned} \tag{21}$$

Note that this is still a MINLP problem, due to the nonlinear objective function and mixed-integer variables. We propose an alternating resource optimization algorithm to optimize the subcarrier allocation and sensor transmit power. Due to the Bernoulli distribution, $\mathbb{E}[\gamma_n(k)] = P[\gamma_n(k) = 1]$, i.e., minimizing the mean square error of state estimation is equivalent to maximizing the probability of successful sensory data transmission. Furthermore, the probability of successful data transmission can be transformed to the probability that the achievable transmission rate of the uplink is no less than the required transmission rate. Then, the problem of optimizing the allocation of subcarriers with given sensor transmit power is simplified as

$$\begin{aligned}
&\mathcal{SP}_{1.1}: \max_{\boldsymbol{\theta}} \sum_{n\in\mathcal{N}} \left(\overline{r_{n,s}(k)} - \frac{\bar{d}_n(k)}{T_{\mathrm{s}}(k)}\right), \forall s \in \mathcal{S} \\
&\text{s.t.} \quad \text{(15a)}, \text{(15b)}, \text{(15h)},
\end{aligned} \tag{22}$$

where $\overline{r_{n,s}(k)} = \theta_{n,s}(k)\bar{b}\log_2(1 + \frac{p_n(k)\overline{h_{n,s}}}{\sigma^2})$, and $\overline{h_{n,s}}$ is the channel power gain averaged over the number of control steps K to reduce the channel randomness, i.e., $\overline{h_{n,s}} = \frac{1}{K}\sum_{k=1}^{K} h_{n,s}(k)$. Problem $\mathcal{SP}_{1.1}$ is a binary linear programming problem, and the Kuhn-Munkres (KM) algorithm is considered effective for binary matching [86]. In this work, the KM algorithm is employed to address the subcarrier allocation problem. We reformulate the problem as a weighted bipartite graph matching problem. Generally, a weighted bipartite graph is defined as $\mathbb{G}(\mathcal{V}, \mathcal{E}, \mathcal{W})$. Here, the set of vertices is denoted as $\mathcal{V} = \mathcal{N} \cup \mathcal{S}$. $\mathcal{E}$ is the set of edges connecting a vertex in set $\mathcal{N}$ and $\mathcal{S}$. $\mathcal{W}$ is the weight of edges. In this work, the weight of the line connecting the vertex n and the vertex s is set as $\overline{r_{n,s}(k)}$. The number of nodes in $\mathcal{N}$ is equal to that in $\mathcal{S}$. Therefore, we can use KM algorithm to transform the weighted matching problem into a combinatorial one for finding a perfect matching and obtaining the optimal solution.

After obtaining the subcarrier allocation, the transmit power optimization problem of sensors could be rewritten as

$$\begin{aligned}
&\mathcal{SP}_{1.2}: \min_{\boldsymbol{p}} \sum_{n\in\mathcal{N}} \left\{p_n(k) + \kappa \max\left\{d_n(k) - r_{n,s}(k)T_{\mathrm{s}}(k), 0\right\}\right\} \\
&\text{s.t.} \quad \text{(15c)},
\end{aligned} \tag{23}$$

where κ is the penalty factor, typically a large positive number. The failure of sensory data transmission is considered as a penalty term to be attached to the objective function.

Remark 1: With insight of $\mathcal{SP}_{1.2}$, it can be seen that (15c) is the power constraint for each sensor and the objective function is the summation operation among all sensors. Besides, the data transmission among sensors does not interfere with each other, thus $\mathcal{SP}_{1.2}$ can be decomposed into N parallel subproblems. Each subproblem aims to optimize the transmit power of one sensor. The derivative of the objective function can be expressed as

$$f'[p_n(k)] = \begin{cases} 1 - \frac{\kappa\theta_{n,s}(k)\bar{b}T_s(k)h_{n,s}(k)}{(\sigma^2 + p_n(k)h_{n,s}(k))\ln(2)}, & \text{if } d_n(k) > r_{n,s}(k)T_{\mathrm{s}}, \\ 1, & \text{otherwise.} \end{cases} \tag{24}$$

It can be observed that when the transmission power $p_n(k)$ is below a certain value, the derivative of the objective function first exhibits negative values, followed by positive values, indicating that the objective function is single-peaked. Therefore, the optimal transmit power of sensors can be obtained via the bisection method.

Until now, the problems $\mathcal{SP}_{1.1}$ and $\mathcal{SP}_{1.2}$ could be successfully solved. Then, the subcarrier allocation and sensor transmit power are optimized alternatively to find the solution of the original problem $\mathcal{SP}_1$ by an iterative method. Subsequently, it can be determined whether the sensory data from sensor n

Algorithm 1: Alternating Resource Optimization Algorithm.

Input: $\mathcal{N}$, $\mathcal{S}$, $T_{\mathrm{s}}(k)$;
Output: $\boldsymbol{\theta}(k)$, $\boldsymbol{p}(k)$;
Initialization: $\tau = 0$, $\boldsymbol{p}(k)$, $fit(\tau) = 0$;
while $\tau \leq \tau_{\max}$ **do**
  $\tau \leftarrow \tau + 1$;
  for Each sensor $n \in \mathcal{N}$ **do**
    for Each subcarrier $s \in \mathcal{S}$ **do**
      Calculate the weight matrix $r_{n,s}(k)$ according to (8);
    end for
  end for
  Subcarrier allocation with KM algorithm;
  Transmit power determination with bisection method;
  Calculate objective function value of $\mathcal{SP}_{1.1}$, denoted as $fit(\tau)$;
  if $fit(\tau) - fit(\tau - 1) < \epsilon$ **then**
    Break;
  end if
end while
Obtain $\mathcal{N}'$ via (9);
$a \leftarrow 0$;
while $|\mathcal{N}'| + a + 1 \leq S$ **do**
  for Each subcarrier $s \in \mathcal{S}$ **do**
    $\theta_{|\mathcal{N}'|+a+1,s} = 0$;
  end for
  $a \leftarrow a + 1$;
end while
Subcarrier allocation with KM algorithm;
for Each sensor $n \in \mathcal{N}'$ **do**
  $\mathcal{S}_n \leftarrow s|\theta_{n,s} == 1$; $\mathcal{S} = \mathcal{S} \backslash \mathcal{S}_n$;
  $r_n^0 \leftarrow \sum_{s \in \mathcal{S}_n} r_{n,s}(k)$;
end for
for Each subcarrier $s \in \mathcal{S}$ **do**
  for Each sensor $n \in \mathcal{N}'$ **do**
    $\mathcal{S}' \leftarrow \mathcal{S}_n \cup s$;
    $r_n^1 \leftarrow \sum_{s' \in \mathcal{S}'} \omega_{n,s'}(k)$; $r_{\Delta,n} \leftarrow r_n^1 - r_n^0$;
  end for
  $n' \leftarrow \arg\max_{n \in \mathcal{N}'} \{r_{\Delta,n}\}$;
  $\theta_{n',s}(k) \leftarrow 1$; $\mathcal{S}_{n'} \leftarrow \mathcal{S}_{n'} \cup s$; $r_{n'}^0 \leftarrow r_{n'}^1$;
end for
return $\boldsymbol{\theta}(k)$, $\boldsymbol{p}(k)$;

is transmitted successfully or not. If the transmission fails, the sensor will not be scheduled. The KM algorithm is employed again for subcarrier reallocation. However, unlike before, the number of sensors is different with that of subcarriers. The set of scheduled sensors is denoted as $\mathcal{N}'$, and $|\mathcal{N}'| < S$. To utilize the KM algorithm, $S - |\mathcal{N}'|$ dummy nodes are added to the set $\mathcal{N}'$ to make the dimension of $\mathcal{N}'$ be equal to that of $\mathcal{S}$. Subsequently, edges between dummy nodes in $\mathcal{N}'$ and nodes in $\mathcal{S}$ are added, with their weights setting to zero. Moreover, the subcarriers matched to the dummy nodes are added to the subcarrier candidate set. The subcarriers in the candidate set are matched to the sensors in $\mathcal{N}'$, and the transmission rate gaps between unallocated subcarriers and allocated subcarriers are calculated. Finally, the subcarrier is allocated to the sensor with the largest transmission rate gap. The original maximum weight matching problem is solved until the candidate set is null. In summary, the alternating resource optimization algorithm for solving the uplink transmission subproblem is summarized in Algorithm 1. The main idea of Algorithm 1 is to allocate subcarriers among sensors and optimize sensor transmit power. Firstly, the weights of edges in the matching matrix are calculated. The corresponding computational complexity is $\mathcal{O}(NS)$. Then, the KM algorithm is used to solve the subcarrier allocation. The corresponding computational complexity is $\mathcal{O}(S^3)$. Subsequently, the bisection method is employed to determine the transmit power of sensors. The corresponding computational complexity is $\mathcal{O}(\log_2 p_{\max})$. The subcarrier allocation and the transmit power are alternately carried out. Once convergence is achieved, the scheduled sensors are identified, and the weights of matching matrix is updated accordingly. Finally, subcarriers are reallocated based on the matrix and identified rate gaps. The corresponding computational complexity is $\mathcal{O}(S^3)$. We assume that the number of iterations for alternating optimization is Φ. Therefore, the computational complexity of Algorithm 1 is $\mathcal{O}(\Phi(NS + S^3 + \log_2 p_{\max}) + S^3)$.

B. Downlink Transmission Optimization for Control Commands

The first item of the objective function of problem $\mathcal{SP}_2$ is the mean square error $\sum_{n\in\mathcal{N}} \mathbb{E}[e_n^{\mathrm{c}}(k)^{\mathrm{T}} e_n^{\mathrm{c}}(k)]$, which could be simplified according to (6). It is denoted as

$$\begin{aligned}\mathbb{E}\left[e_n^{\mathrm{c}}(k)^{\mathrm{T}} e_n^{\mathrm{c}}(k)\right] &= u_n^{\mathrm{c}}(k)^{\mathrm{T}} u_n^{\mathrm{c}}(k) - u_n^{\mathrm{c}}(k)^{\mathrm{T}} u_n^{\mathrm{c}}(k) \mathbb{E}\left[\nu_n(k)\right] \\ &= u_n^{\mathrm{c}}(k)^{\mathrm{T}} u_n^{\mathrm{c}}(k) \left\{1 - \mathbb{E}\left[\nu_n(k)\right]\right\}. \end{aligned} \tag{25}$$

Similar to the calculation of $\mathbb{E}[\gamma_n(k)]$, $\mathbb{E}[\nu_n(k)]$ could be rewritten as

$$\begin{aligned}\mathbb{E}\left[\nu_n(k)\right] &= \Pr\left\{\sum_{m\in\mathcal{M}} \varphi_{n,m}(k) \underline{b}_m(k) \right. \\ &\qquad \left. \log_2\left(1 + \frac{h_n(k) q_m(k)}{\sigma^2}\right)\right\} \geq \frac{\sum_{n\in\mathcal{N}_m} \underline{d}_n(k)}{T_{\mathrm{a}}(k)} \\ &= \exp\left\{-\frac{\sigma^2\left[2^{\frac{\sum_{n\in\mathcal{N}_m} \underline{d}_n(k)}{T_{\mathrm{a}}(k)\sum_{m\in\mathcal{M}} \varphi_{n,m}(k)\underline{b}_m(k)}} - 1\right]}{2\sum_{m\in\mathcal{M}} \varphi_{n,m}(k) q_m(k)}\right\}. \end{aligned} \tag{26}$$

Therefore, problem $\mathcal{SP}_2$ can be rewritten as

$$\begin{aligned}&\min_{M,\boldsymbol{\varphi},\underline{\boldsymbol{b}},\boldsymbol{q}} \sum_{n\in\mathcal{N}} u_n^{\mathrm{c}}(k)^{\mathrm{T}} u_n^{\mathrm{c}}(k)\{1 - \mathbb{E}\left[\nu_n(k)\right]\} + \beta_2 E_2(k) \\ &\text{s.t.} \quad \text{(15d)}, \text{(15e)}, \text{(15f)}, \text{(15g)}, \text{(15i)}. \end{aligned} \tag{27}$$

After analysis, it is evident that the problem is a MINLP problem due to the nonlinear objective function and mixed-integer variables, which is difficult to solve optimally. Consider a two-step solution process, in the first step, the multicast grouping problem is solved with given bandwidth and power allocation. Then, in the second step, we obtain the bandwidth and power allocation by solving resource allocation problem with the given actuator group.

1) Multicast Grouping Problem: Analysis of the objective function of multicast grouping problem reveals the need to maximize $\sum_{n\in\mathcal{N}}\sum_{m\in\mathcal{M}}\varphi_{n,m}\mathbb{E}[\nu_n(k)]$. The goal is to group a set of points $\varepsilon_1,\varepsilon_2,\ldots,\varepsilon_N$ into clusters $\mathcal{N}_1,\mathcal{N}_2,\ldots,\mathcal{N}_M$. Multicast group division is performed based on the probability $\mathbb{E}[\nu_n(k)]$, which is impacted by channel conditions and transmission demands of different actuators. As $\sum_{n\in\mathcal{N}}\mathbb{E}[\nu_n(k)]$ is a constant and $\sum_{m\in\mathcal{M}}\varphi_{n,m}(k)=1$, the objective function could be transformed to

$$\begin{aligned}\min_{M,\boldsymbol{\varphi}} &\sum_{n\in\mathcal{N}}\mathbb{E}\left[\nu_n(k)\right]\sum_{m\in\mathcal{M}}\varphi_{n,m}(k)\\ &-\sum_{m\in\mathcal{M}}\sum_{n\in\mathcal{N}}\left\{\varphi_{n,m}(k)\min_{n\in\mathcal{N}_m}\mathbb{E}\left[\nu_n(k)\right]\right\}\\ =&\sum_{m\in\mathcal{M}}\sum_{n\in\mathcal{N}}\varphi_{n,m}(k)\left\{\mathbb{E}\left[\nu_n(k)\right]-\min_{n\in\mathcal{N}_m}\mathbb{E}\left[\nu_n(k)\right]\right\},\end{aligned}\tag{28}$$

$\sum_{n\in\mathcal{N}}\varphi_{n,m}(k)\{\mathbb{E}[\nu_n(k)]-\min_{n\in\mathcal{N}_m}\mathbb{E}[\nu_n(k)]\}$ could be rewritten as the distance between an actuator point $\varepsilon_n=\mathbb{E}[\nu_n(k)]$ and a center point $\underline{\varepsilon}_m=\min_{n\in\mathcal{N}_m}\varepsilon_n$ of group m. Then, multicast grouping problem could be regarded as a clustering problem, and the objective of the problem is expressed as

$$\min_{M,\boldsymbol{\varphi}}\sum_{m\in\mathcal{M}}\sum_{n\in\mathcal{N}_m}|\varepsilon_n-\underline{\varepsilon}_m|.\tag{29}$$

The multicast grouping problem could be simplified as

$$\begin{aligned}\mathcal{SP}_{2.1}:\min_{M,\boldsymbol{\varphi}}&\sum_{m\in\mathcal{M}}\sum_{n\in\mathcal{N}_m}|\varepsilon_n-\underline{\varepsilon}_m|\\ &\text{s.t. (15f), (15g), (15i).}\end{aligned}$$

We solve this clustering problem using a heuristic algorithm that involves two layers of iterations, as shown in Algorithm 2. The outer iteration automatically determines the number of groups by a clustering evaluation metric called the silhouette coefficient. A clustering algorithm is employed in the inner iteration to determine the actuators grouping, due to its advantages such as fast convergence and better clustering results.

1) Outer Iteration: The silhouette coefficient is introduced as an internal index for evaluating the effectiveness of clustering. It quantifies the similarity between a target and its own cluster, relative to other clusters, on a scale from -1 to 1. A larger value of this coefficient indicates that the target has a higher degree of matching relationship with its own cluster and a lower degree of matching relationship with other clusters. Therefore, the larger this value is, the better the clustering result is. The silhouette

Algorithm 2: Multicast Grouping Algorithm.

Input: $\boldsymbol{\varepsilon}=\{\varepsilon_1,\varepsilon_2,\ldots,\varepsilon_N\}$, δ;
Output: M^*, $\mathcal{N}_m$;
Initialization: $M=\lceil\sqrt{N}\rceil$, $\xi^*=-\infty$;
repeat
  Choose M elements far from each other in $\boldsymbol{\varepsilon}$ as the cluster centers $\underline{\varepsilon}_m$;
  repeat
    for Each sensor $n\in\mathcal{N}$ **do**
      for Each group $m\in\mathcal{M}$ **do**
        $\Delta_{nm}=|\varepsilon_n-\underline{\varepsilon}_m|$;
      end for
      $m=\arg\min_m\{\Delta_{n1},\ldots,\Delta_{nm}\}$;
      Cluster ε_n into $\mathcal{N}_m$;
    end for
    Update new $\underline{\varepsilon}'_m$ as $\min_{n\in\mathcal{N}_m}\varepsilon_n$;
  until $|\underline{\varepsilon}'_m-\underline{\varepsilon}_m|<\delta,\ \forall m$;
  Calculate the silhouette coefficient $\xi(M)$ according to (33);
  if $\xi(M)>\xi^*$ **then**
    $M^*=M$;
    $\xi^*=\xi(M)$;
  end if
  $M\leftarrow M-1$;
until $M=1$;
return M^* and $\mathcal{N}_m$;

coefficient for sample i is calculated as [87]

$$\xi(i)=\frac{R(i)-F(i)}{\max\{R(i),F(i)\}},\forall i\in\mathcal{N},\tag{30}$$

where $F(i)$ and $R(i)$ are the degrees of cohesion and isolation, which reflect the closeness of a sample point to the in-cluster and out-of-cluster elements, respectively. They are calculated as

$$F(i)=\frac{1}{N_m-1}\sum_{j\neq i}^{N_m}\text{dist}(i,j),i,j\in\mathcal{N}_m,\tag{31}$$

$$R(i)=\min_{m'\neq m}\frac{1}{N_{m'}}\sum_{j\in\mathcal{N}_{m'}}\text{dist}(i,j),i\in\mathcal{N}_m,j\in\mathcal{N}_{m'},\tag{32}$$

where m' is the group in M excluding the group to which sample i belongs, N_m is the number of actuators in group m, and $\text{dist}(i,j)$ is the distance between sample i and sample j. The average silhouette coefficient of the clustering result is denoted as

$$\xi=\frac{1}{N}\sum_{i\in\mathcal{N}}\xi(i).\tag{33}$$

According to the result in [88], there exists an optimal value M^*, which is less than $\sqrt{N}$. Therefore, we initially set the value of M as $\lceil\sqrt{N}\rceil$, where $\lceil\cdot\rceil$ indicates the ceil operation. Then, the actuators are divided into M groups using the clustering algorithm to be introduced below. By iterating through the number of groups in the outer loop, the number of groups corresponding

to the maximum average profile coefficient value is selected as M^*.

1) Inner Iteration: Conventional K-means++ algorithms can not be directly applied due to the differences in center selection and distance calculation. In traditional algorithms, cluster centers are typically the arithmetic mean of points, whereas in our approach, the center is the minimum of the points, enhancing computational efficiency. Additionally, we use the 1-norm, rather than the 2-norm, due to the lower complexity when handling one-dimensional data [89]. Therefore, a modified K-means++ algorithm can be used to solve the clustering problem and the general procedure of the algorithm is as follows. Select M samples from the dataset as the initial clustering centers. Then, convert the shortest distance between each sample and the existing clustering centers into probabilities, and select the next clustering center according to roulette wheel selection method. Afterwards, for each sample ε_n in the dataset, calculate its distance to the M clustering centers and classify it into the cluster corresponding to the clustering center with the smallest distance. Finally, update the clustering centers, and repeat the above steps until the positions of the clustering centers no longer change.

The complexity of the K-means++ clustering algorithm is $O(NM)$, where N is the number of samples. Since we search M from 1 to $\sqrt{N}$, the computational complexity of Algorithm 2 is given by $O(N\sum_{M=1}^{\sqrt{N}} M) = O(N^2)$.

2) Bandwidth and Power Allocation: With given division of multicast groups, the problem of bandwidth and power allocation for each group could be rewritten as

$$\mathcal{SP}_{2.2}: \min_{\underline{\boldsymbol{b}},\boldsymbol{q}} \sum_{n\in\mathcal{N}} u_n^{\mathrm{c}}(k)^{\mathrm{T}} u_n^{\mathrm{c}}(k)\{1-\mathbb{E}\left[\nu_n(k)\right]\}+\beta_2 E_2(k)$$
$$\text{s.t.} \quad \text{((15d), (15e).} \tag{34}$$

When the bandwidth $\rho_m(k)B$ is allocated to group m, the transmission rate of group m can be expressed as

$$r_{m,\mathrm{B}}(k) = \rho_m(k) B \log_2\left(1+\min_{n\in\mathcal{N}_m}\Gamma_{n,m}(k)\right), \forall m\in\mathcal{M}, \tag{37}$$

where $\rho_m(k)$ is the bandwidth allocation factor. The transmission delay of actuators in group m is expressed as $t_{m,\mathrm{B}}(k) = \frac{\sum_{n\in\mathcal{N}_m}\underline{d}_n(k)}{r_{m,\mathrm{B}}(k)}$. The downlink control error is only affected by the probability of successful transmission of downlink control commands. Then, the bandwidth allocation problem for a given transmit power can be simplified as

$$\mathcal{SP}_{2.2}^1: \min_{\rho_m(k)} \max_m \frac{1}{\rho_m(k)} t_{m,\mathrm{B}}(k) \tag{38}$$
$$\text{s.t.} \sum_{m\in\mathcal{M}} \rho_m(k) \le 1, \tag{38a}$$
$$0<\rho_m(k)<1, m\in\mathcal{M}. \tag{38b}$$

Since $\mathcal{M}$ is a convex set and the operation of taking the maximum for variable m is a convexity-preserving operation, $\max_m \frac{1}{\rho_m(k)} t_{m,\mathrm{B}}(k)$ is a convex function. Problem $\mathcal{SP}_{2.2}^1$ is convex due to the convex objective function and the linear constraints. Therefore, it can be solved by a standard convex optimization solver.

Then, with given bandwidth allocation, the transmit power allocation problem can be expressed as

$$\mathcal{SP}_{2.2}^2: \min_{\boldsymbol{q}} \sum_{n\in\mathcal{N}} \mathbb{E}\left[e_n^{\mathrm{c}}(k)^{\mathrm{T}} e_n^{\mathrm{c}}(k)\right] + \beta_2 E_2(k)$$
$$\text{s.t.(15e).} \tag{39}$$

The first and second order derivatives of the objective function with respect to $\boldsymbol{q}$ could be expressed respectively as (35) and (36) shown at the bottom of this page, where $H_m(k) = \log_2(1+\min_{n\in\mathcal{N}_m}\frac{h_n(k)q_m(k)}{\sigma^2})$. It can be seen that the function $H_m(k)$ is convex due to its non-negative second-order derivative with respect to $\boldsymbol{q}$. Coupled with the convexity constraint (15e), the problem is a convex optimization problem. Therefore, it can be solved efficiently by a standard convex optimization solver. Finally, the solution to problem $\mathcal{SP}_2$ is obtained by alternately optimising the bandwidth allocation and AP transmit power.

In summary, the original problem is a MINLP problem, making its optimal solution difficult to obtain. As a solution, the original problem is divided into two subproblems with a given division point η, i.e., the uplink transmission subproblem and the downlink transmission subproblem. Both subproblems are non-convex. The objective function of the former is transformed based on the properties of Bernoulli distribution, enabling optimal solution using Algorithm 1. The latter is further split

$$\frac{\partial L\left(\sum_{n\in\mathcal{N}}\mathbb{E}\left[e_n^{\mathrm{c}}(k)^{\mathrm{T}}e_n^{\mathrm{c}}(k)\right]+\beta_2E_2(k)\right)}{\partial q_m(k)} = \frac{\beta_2\sum_{n\in\mathcal{N}_m}\underline{d}_n(k)}{\underline{b}_m(k)H_m(k)} - q_m(k)\frac{\beta_2\sum_{n\in\mathcal{N}_n}\underline{d}_n(k)}{\left(\underline{b}_m(k)H_m(k)\right)^2}\cdot\frac{\underline{b}_m(k)}{\ln(2)}\cdot\frac{\min_{n\in\mathcal{N}_m}\frac{h_n(k)}{\sigma^2}}{1+\min_{n\in\mathcal{N}_m}\frac{h_n(k)q_m(k)}{\sigma^2}}, \tag{35}$$

$$\frac{\partial^2 L\left(\sum_{n\in\mathcal{N}}\mathbb{E}\left[e_n^{\mathrm{c}}(k)^{\mathrm{T}}e_n^{\mathrm{c}}(k)\right]+\beta_2E_2(k)\right)}{\partial q_m^2(k)} = \frac{\beta_2\sum_{n\in\mathcal{N}_n}\underline{d}_n(k)\min_{n\in\mathcal{N}_m}\frac{h_n(k)}{\sigma^2}}{\ln(2)\underline{b}_m(k)H_m^2(k)\left(1+\min_{n\in\mathcal{N}_m}\frac{h_n(k)q_m(k)}{\sigma^2}\right)}$$
$$\left\{\frac{\min_{n\in\mathcal{N}_m}\frac{h_n(k)}{\sigma^2}}{H_m(k)\left(1+\min_{n\in\mathcal{N}_m}\frac{h_n(k)q_m(k)}{\sigma^2}\right)}\left[1+\frac{1+H_m(k)}{\underline{b}_m(k)H_m(k)}\right]-1-\frac{1}{\underline{b}_m(k)H_m(k)}\right\}. \tag{36}$$

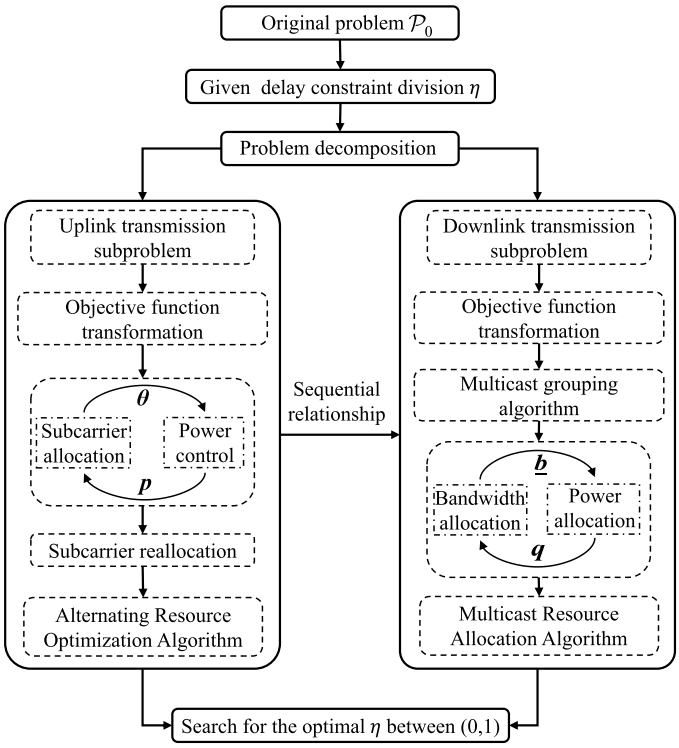

Fig. 2. The diagram of solution process.

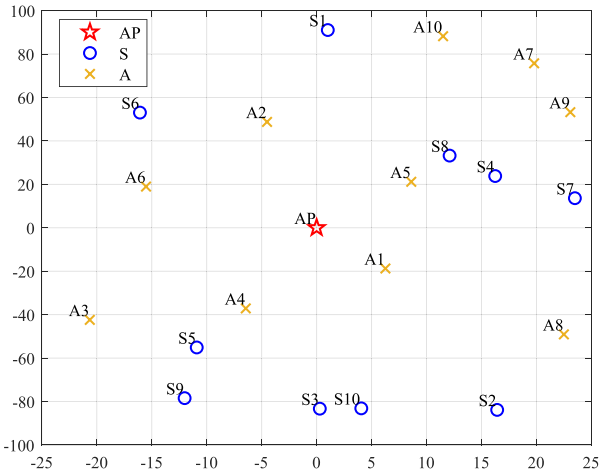

Fig. 3. Network topology, where "S" denotes sensor, and "A" denotes actuator.

TABLE II
MAIN PARAMETERS

Parameters	Values
Transmission bandwidth B	1.4 MHz
Noise power σ^2	-42 dBm
The duration of one control step T	100 ms
Average packet length of sensory data $\bar{d}_n$	6 Kbits
Range of packet lengths of control commands $\underline{d}_n$	$(450, 1100)$ bits
Maximum transmit power of sensor $p_{\max}$	12 dBm
Maximum transmit power of AP $q_{\max}$	18 dBm

into two sub-problems, the multicast grouping problem and the resource allocation problem. The former can be addressed using Algorithm 2, while the latter can be decomposed into two convex problems and iteratively solved using a standard convex optimization solver. After solving the above two subproblems, we can obtain the minimum value of the overall cost for the given η. Then, search for η in (0,1) to obtain the solution to $\mathcal{P}_0$. The detailed solution process is shown as Fig. 2.

V. Performance Evaluation

In this paper, the proposed transmission and control integrated design (TCID) scheme aims to reduce the overall cost of the considered cyber-physical system. In this section, we perform extensive simulations to evaluate the performance of TCID in terms of the overall cost, control cost and uplink-downlink communication cost. Three additional schemes are considered as comparing ones. The first one is transmission and control integrated design scheme for uplink bandwidth allocation (TCID-UBA), where resource allocation for uplink transmission focuses on bandwidth allocation rather than subcarrier allocation, and multicast transmission is adopted for the downlink. The second one is transmission and control integrated design scheme for downlink broadcasting (TCID-DB) transmission, in which OFDMA with subcarrier allocation is employed for uplink transmission. The third one is transmission and control integrated design scheme for downlink unicast (TCID-DU) transmission, specifically using OFDMA, where OFDMA with subcarrier allocation is employed for uplink transmission.

In the simulation, the performance comparison is evaluated according to the network topology covering a rectangular area $[-25, 25]_{\mathrm{m}} \times [-100, 100]_{\mathrm{m}}$, where $N = 10$ sensor-actuator pairs are placed and the AP is located at $(0, 0)$ m, as shown in Fig. 3. Moreover, we employ MATLAB as the programming platform and utilize the CVX toolbox for solving convex optimization problems. The main parameters used in the simulation are shown in Table II.

A. Performance Comparison With Different Schemes

The performance comparison among four schemes in terms of the overall cost, control cost, and communication cost is presented in Fig. 4. For the uplink transmission, TCID scheme achieves a 68% reduction in overall cost compared to TCID-UBA scheme. This advantage results from the use of subcarrier allocation, which allows finer control over resource allocation by utilizing channel heterogeneity compared to bandwidth allocation. For the downlink transmission, TCID scheme reduces overall cost by 15% and 90% compared to TCID-DU and TCID-DB schemes, respectively. This significant improvement is primarily due to the multicast transmission mechanism employed in the downlink. Compared to unicast, multicast minimizes resource consumption, and unlike broadcast, it targets only relevant devices, improving overall efficiency. Fig. 4(b) and (c) show that both the control cost and the communication cost with TCID-DU and TCID-UBA schemes are higher than those with the proposed scheme. Moreover, the downlink broadcast transmission of TCID-DB scheme causes a higher downlink communication cost compared to the proposed scheme. Furthermore, the communication cost with TCID-DU and TCID-UBA schemes is significantly higher due to increased transmission

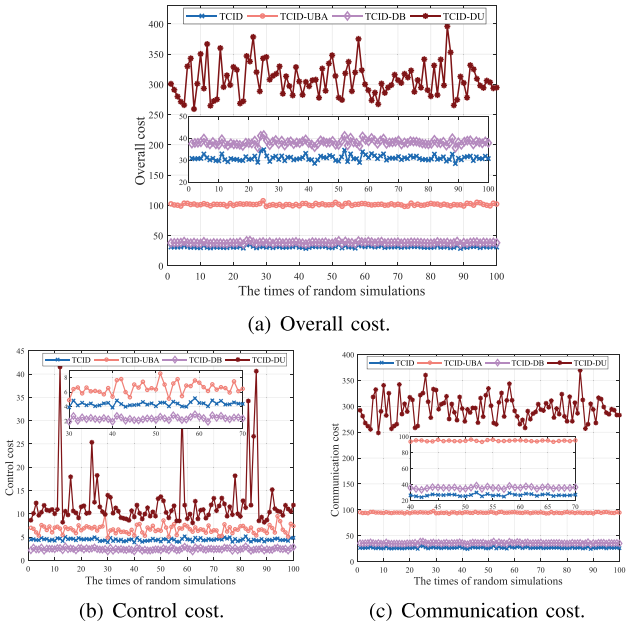

(a) Overall cost.

(b) Control cost.

(c) Communication cost.

Fig. 4. Performance comparison among different approaches.

latency. This results from the inefficiency of downlink unicast transmission and the bandwidth allocation strategy which limits resource utilization and increases overhead. In summary, Fig. 4 clearly demonstrates that the performance improvement is attributed to its superior adaptive capability to the control system dynamics and wireless channel heterogeneities compared to other three schemes. The proposed scheme achieves efficient control scheduling and collaborative uplink-downlink transmission. Additionally, it enhances resource utilization through joint time-frequency resources optimization, which mitigates the impact of wireless resources scarcity on control performance.

B. Performance Comparison With Different Parameters

Without loss of generality, we then conducted a comparative study with different network settings. The effect of the number of sensor-actuator pairs on system performance is shown in Fig. 5. It can be seen that all three costs increase with the number of sensor-actuator pairs for all schemes. Fig. 5(a) shows that the overall cost with the proposed scheme is consistently lower than that with other compared ones, and the rate of increase is significantly smaller compared with TCID-DU and TCID-UBA schemes. The reason is that, if the system consists of more sensor-actuator pairs, more state and control information needs to be transmitted to the controllers and actuators, leading to higher communication cost. In addition, the control cost also increases with the number of sensor-actuator pairs due to the accumulation of sensing error from sensors and control error from actuators caused by unsuccessful data transmission. Fig. 5(b) reveals that as the number of sensor-actuator pairs increases, the use of unicast transmission in the downlink results in the inability to meet the transmission latency requirements of some actuators with worse channel conditions. Consequently, the success rate of control command transmission is reduced, leading to a significant increase in the control cost with TCID-DU scheme. In contrast, the use of multicast or broadcast transmission in the downlink can significantly reduce the cost, and thus the control costs with other three schemes are relatively low and increase relatively slowly. Fig. 5(c) shows that the proposed scheme can considerably mitigate the increase of communication cost as the number of sensor-actuator pairs grows, since its information transmission design optimizes resource allocation and reduces redundant transmissions.

The effect of transmission bandwidth on system performance is shown in Fig. 6. With the growth of bandwidth, each sensor/actuator can be allocated more bandwidth resources, which in turn increases the data transmission rate. This reduces transmission delay and improves the probability of successful data transmission, resulting in a decrease in all three costs. At lower transmission bandwidths (0.8 MHz to 1.6 MHz), increasing bandwidth leads to a significant reduction in all three costs. However, at higher bandwidths (1.6 MHz to 2 MHz), the reduction in costs becomes less noticeable. Fig. 6(a) shows that the overall cost with TCID scheme is consistently lower than that with other three schemes. Fig. 6(b) and (c) show that the control cost and communication cost with both TCID-DU and TCID-UBA schemes decrease substantially with the increase of transmission bandwidth. This reduction is due to two factors: the higher transmission rates for actuators enabled by additional bandwidth allocated for downlink unicast, and the increased availability of bandwidth for uplink bandwidth allocation.

The effect of the duration of one control cycle on system performance is shown in Fig. 7. With the growth of one control cycle duration, the latency requirement for sensory information and control command transmission gradually decreases. Fig. 7(a) shows that when the duration of one control cycle grows, the overall cost with all four schemes decreases. Among four schemes, TCID scheme exhibits the lowest overall cost and the largest reduction in cost. Fig. 7(b) and (c) show that as the duration of one control cycle increases, the delay requirement for data transmission decreases, allowing more sensors and actuators to successfully transmit data. Therefore, the reduction in control cost becomes more significant. In this context, the downlink unicast transmission of TCID-DU scheme results in worse channel conditions and higher transmission delay for some actuators. As a result, the reduction in delay requirements has a smaller impact on control cost compared with other three schemes. However, since the number of sensors and actuators increases, the energy consumed by the sensors and controllers also increases.

By optimizing the uplink-downlink division point and designing the transmission method for both phases, the proposed scheme achieves a more effective trade-off between control cost and communication cost. Specifically, the scheme achieves a significant reduction in control cost at a slow decreasing of communication cost, with the ultimate goal of obtaining the lowest overall cost. This demonstrates the advantages of the proposed scheme in reducing the overall cost.

The impact of the uplink-downlink duration division point on the performance is shown in Fig. 8. Fig. 8(a) shows that the decreasing delay requirement for uplink transmission leads to a rapid reduction in uplink cost. However, when the delay reaches a certain point, the effect of the reduced delay requirement

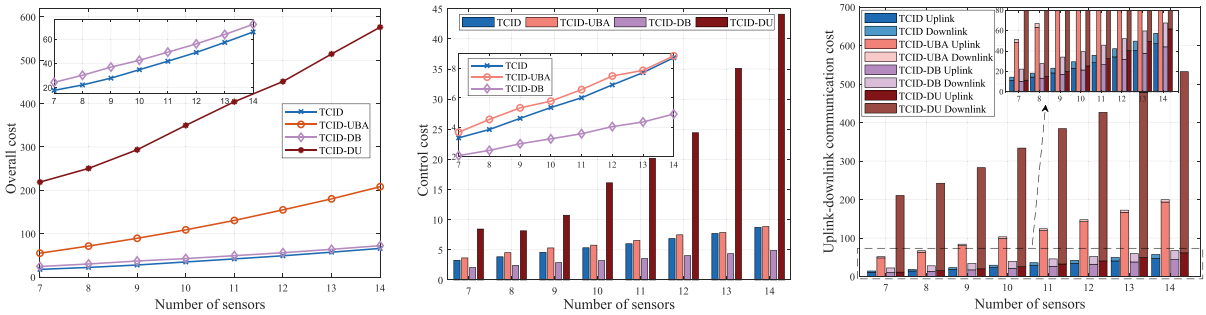

(a) Overall cost. (b) Control cost. (c) Uplink-downlink communication cost.

Fig. 5. Performance comparison with different numbers of sensors.

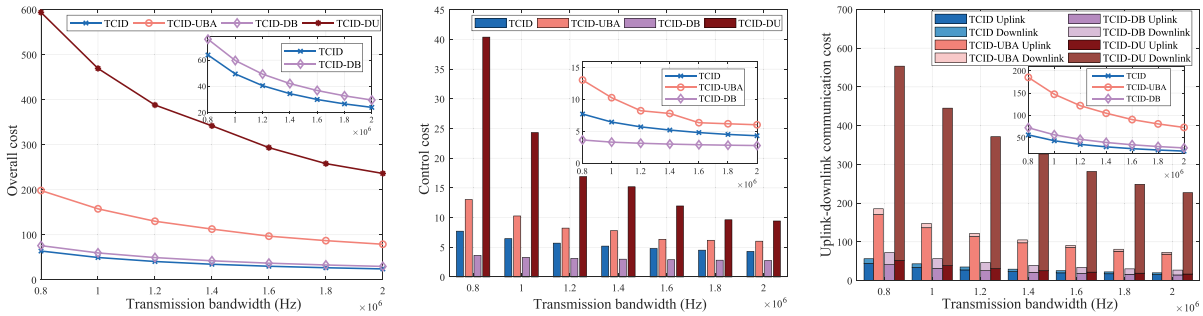

(a) Overall cost. (b) Control cost. (c) Uplink-downlink communication cost.

Fig. 6. Performance comparison with different transmission bandwidths.

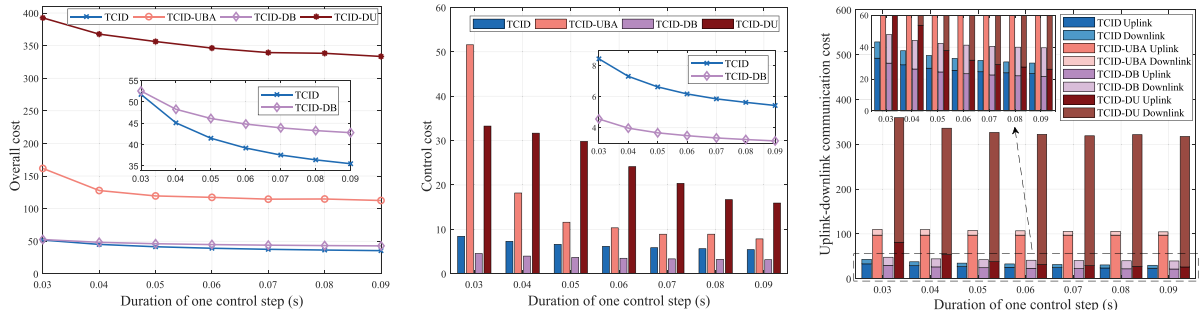

(a) Overall cost. (b) Control cost. (c) Uplink-downlink communication cost.

Fig. 7. Performance comparison with different durations of one control step.

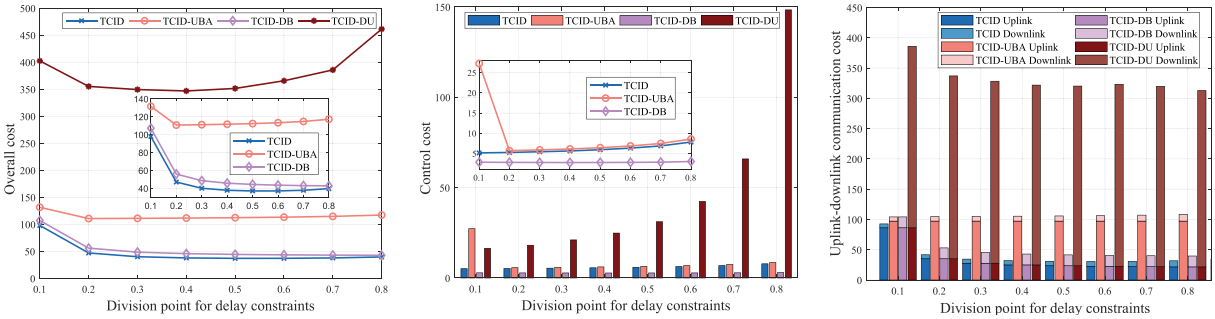

(a) Overall cost. (b) Control cost. (c) Uplink-downlink communication cost.

Fig. 8. Performance comparison with different uplink-downlink duration division points.

on further reducing uplink cost diminishes. Conversely, the downlink cost gradually increases due to the higher requirement for downlink transmission. The optimal uplink-downlink duration division points vary among four schemes, indicating that there exists an optimal uplink-downlink delay allocation approach for each scheme. Fig. 8(b) shows that the control cost with TCID-DU scheme is mainly the downlink control cost resulting from the downlink unicast transmission. Consequently, the control cost of this scheme gradually increases with the growth of uplink-downlink duration division point, even a sharp increase after the division point reaches 0.6. Since TCID scheme proposed in this paper employs multicast transmission for the downlink, the control cost increases very slowly with different uplink-downlink duration division points. As shown in Fig. 8(c), the uplink communication cost with TCID-UBA scheme, which uses bandwidth allocation to allocate uplink resources, constitutes over 90% of communication cost. In contrast, for TCID-DU scheme, which employs unicast transmission while the other three schemes use broadcast or multicast, the downlink communication cost constitutes nearly 90% of the communication cost.

With the growth of uplink-downlink duration division point, the uplink communication cost for all four schemes decreases, while the downlink communication cost increases. These trends emphasize the significance of integratedly designing uplink-downlink transmission and control.

VI. Conclusion

In this paper, we have proposed a multicast uplink-downlink transmission scheme for the latency-critical full-loop control in cyber-physical systems. The explored impact of uplink sensing information and downlink control information transmission on the full-loop control performance provides a cornerstone for the integrated design of communication and control to enhance the overall performance. The proposed scheme can flexibly allocate resources based on the dynamics of the system and heterogeneous channel conditions, effectively minimizing the overall cost. Moreover, it can also significantly reduce the header overhead of small packets by aggregating multiple actuators into a single multicast group, making it highly suitable for the control information transmission in cyber-physical systems. For the future work, we will study the transmission resource allocation for cyber-physical systems with heterogeneous tasks.

References

[1] K. Zhang, Y. Shi, S. Karnouskos, T. Sauter, H. Fang, and A. W. Colombo, "Advancements in industrial cyber-physical systems: An overview and perspectives," *IEEE Trans. Ind. Informat.*, vol. 19, no. 1, pp. 716–729, Jan. 2023.

[2] Z. Cai and X. Zheng, "A private and efficient mechanism for data uploading in smart cyber-physical systems," *IEEE Trans. Netw. Sci. Eng.*, vol. 7, no. 2, pp. 766–775, Apr.–Jun. 2020 .

[3] M. Afrin, J. Jin, A. Rahman, A. Gasparri, Y.-C. Tian, and A. Kulkarni, "Robotic edge resource allocation for agricultural cyber-physical system," *IEEE Trans. Netw. Sci. Eng.*, vol. 9, no. 6, pp. 3979–3990, Nov./Dec. 2022.

[4] Y. Dai et al., "A survey of graph-based resource management in wireless networks -Part I: Optimization approaches," *IEEE Trans. Cogn. Commun. Netw.*, vol. 11, no. 4, pp. 2078–2100, Aug. 2025.

[5] J. Zhou, L. Li, A. Vajdi, X. Zhou, and Z. Wu, "Temperature-constrained reliability optimization of industrial cyber-physical systems using machine learning and feedback control," *IEEE Trans. Autom. Sci. Eng.*, vol. 20, no. 1, pp. 20–31, Jan. 2023.

[6] Z. Ji, C. Chen, S. Zhu, Y. Ma, and X. Guan, "Intelligent edge sensing and control co-design for industrial cyber-physical system," *IEEE Trans. Signal Inf. Process. Netw.*, vol. 9, pp. 175–189, 2023.

[7] Y. Ma et al., "Smart actuation for end-edge industrial control systems," *IEEE Trans. Autom. Sci. Eng.*, vol. 21, no. 1, pp. 269–283, Jan. 2024.

[8] N. Cheng et al., "Space/aerial-assisted computing offloading for IoT applications: A learning-based approach," *IEEE J. Sel. Areas Commun.*, vol. 37, no. 5, pp. 1117–1129, May 2019.

[9] B. Ma, M. Lin, B. Zhao, H. Ouyang, and J. Wang, "Robust beamforming for communication and control co-design in multi-loop wireless control system," *IEEE Commun. Lett.*, vol. 29, no. 3, pp. 423–427, Mar. 2025.

[10] L. Lyu, L. Zhao, and Y. Dai, "AoI-based priority-aware transmission scheduling for state estimation in industrial IoT systems," in *Proc. 5th Int. Conf. Commun., Signal Process., their Appl.*, 2022, pp. 1–6.

[11] Z. Qiao, L. Lyu, Y. Dai, N. Cheng, and X. Shen, "Energy-aware sensor scheduling and opportunistic transmission for state estimation in industrial IoT systems," in *Proc. IEEE/CIC Int. Conf. Commun. China*, 2023, pp. 1–6.

[12] T. Chang, X. Cao, and W. X. Zheng, "A lightweight sensor scheduler based on AoI function for remote state estimation over lossy wireless channels," *IEEE Trans. Autom. Control*, vol. 69, no. 3, pp. 1697–1704, Mar. 2024.

[13] Z. Zhang, Q. Li, J. Yv, and Z. Ren, "Finite-time robust cooperative distributed estimate with sensor network," *IEEE Sensors J.*, vol. 24, no. 9, pp. 14737–14749, May 2024.

[14] D. Yu, M. Yang, Y.-J. Liu, Z. Wang, and C. L. P. Chen, "Adaptive fuzzy tracking control for uncertain nonlinear systems with multiple actuators and sensors faults," *IEEE Trans. Fuzzy Syst.*, vol. 31, no. 1, pp. 104–116, Jan. 2023.

[15] X. Wen et al., "Age-of-task-aware co-design of sampling, scheduling, and control for industrial IoT systems," *IEEE Internet Things J.*, vol. 11, no. 3, pp. 4227–4242, Feb. 2024.

[16] Z. Wang, Y. Gao, C. Fang, L. Liu, D. Zeng, and M. Dong, "State-estimation-based control strategy design for connected cruise control with delays," *IEEE Syst. J.*, vol. 17, no. 1, pp. 99–110, Mar. 2023.

[17] L. Lyu, C. Chen, C. Hua, S. Zhu, and X. Guan, "Co-design of stabilisation and transmission scheduling for wireless control systems," *IET Control Theory Appl.*, vol. 11, no. 11, pp. 1767–1778, 2017.

[18] X. Wang et al., "RadioDiff: An effective generative diffusion model for sampling-free dynamic radio map construction," *IEEE Trans. Cogn. Commun. Netw.*, vol. 11, no. 2, pp. 738–750, Apr. 2025.

[19] Y. Dai et al., "A survey of graph-based resource management in wireless networks—Part II: Learning approaches," *IEEE Trans. Cogn. Commun. Netw.*, vol. 11, no. 4, pp. 2101–2122, Aug. 2025.

[20] G. Zhang, Y. Lu, M. Li, Z. Zhong, and T. Q. S. Quek, "Joint uplink and downlink robust transmission for cell-free networks," *IEEE Trans. Wireless Commun.*, vol. 23, no. 10, pp. 15308–15321, Oct. 2024.

[21] G. Lee, H. Lee, D. Kim, J. Chung, A. L. Swindlehurst, and J. Choi, "Joint downlink and uplink optimization for RIS-aided FDD MIMO communication systems," *IEEE Trans. Wireless Commun.*, vol. 23, no. 8, pp. 9059–9071, Aug. 2024.

[22] H. Zeng, X. Zhu, Y. Jiang, Z. Wei, S. Sun, and X. Xiong, "Toward UL-DL rate balancing: Joint resource allocation and hybrid-mode multiple access for UAV-BS-assisted communication systems," *IEEE Trans. Commun.*, vol. 70, no. 4, pp. 2757–2771, Apr. 2022.

[23] X.-Y. Zhang and G.-H. Yang, "Distributed secure state estimation for cyber-physical systems under false data injection attacks," *IEEE Trans. Netw. Sci. Eng.*, vol. 11, no. 5, pp. 4443–4455, Sep./Oct. 2024.

[24] W. Chen, Z. Wang, J. Hu, H. Dong, and G.-P. Liu, "Distributed resilient state estimation for cyber-physical systems against bit errors: A zonotopic set-membership approach," *IEEE Trans. Netw. Sci. Eng.*, vol. 10, no. 6, pp. 3922–3932, Nov./Dec. 2023.

[25] W. Yang, W. Luo, and X. Zhang, "Distributed secure state estimation under stochastic linear attacks," *IEEE Trans. Netw. Sci. Eng.*, vol. 8, no. 3, pp. 2036–2047, Jul.–Sep. 2021.

[26] L. Xin, G. He, and Z. Long, "Secure state estimation for multi-sensor cyber-physical systems using virtual sensor and deep reinforcement learning under multiple attacks on major sensor," *IEEE Trans. Netw. Sci. Eng.*, vol. 12, no. 3, pp. 1470–1481, May/Jun. 2025.

[27] N. He, Y. Li, H. Li, D. He, and F. Cheng, "PID-based event-triggered MPC for constrained nonlinear cyber-physical systems: Theory and application," *IEEE Trans. Ind. Electron.*, vol. 71, no. 10, pp. 13103–13112, Oct. 2024.

[28] M. H. Mamduhi, D. Maity, J. S. Baras, and K. H. Johansson, "A cross-layer optimal co-design of control and networking in time-sensitive cyber-physical systems," *IEEE Control Syst. Lett.*, vol. 5, no. 3, pp. 917–922, Jul. 2021.

[29] W. Lucia, G. Franze, and B. Sinopoli, "A supervisor-based control architecture for constrained cyber-physical systems subject to network attacks," *IEEE Trans. Control Netw. Syst.*, vol. 10, no. 3, pp. 1184–1194, Sep. 2023.

[30] H. Ren, Y. Long, H. Li, and T. Huang, "Data-driven group formation control of cyber-physical systems via distributed cloud computing," *IEEE Trans. Ind. Cyber- Phys. Syst.*, vol. 3, pp. 341–350, 2025.

[31] A. Fu and J. A. McCann, "Dynamic decentralized periodic event-triggered control for wireless cyber–physical systems," *IEEE Trans. Control Syst. Technol.*, vol. 29, no. 4, pp. 1783–1790, Jul. 2021.

[32] Z. Ji, C. Chen, J. He, S. Zhu, and X. Guan, "Edge sensing and control co-design for industrial cyber-physical systems: Observability guaranteed method," *IEEE Trans. Cybern.*, vol. 52, no. 12, pp. 13350–13362, Dec. 2022.

[33] H. Ren, Y. Long, H. Ma, and H. Li, "Distributed group coordination of random communication constrained cyber-physical systems using cloud edge computing," *IEEE Trans. Ind. Cyber- Phys. Syst.*, vol. 2, pp. 196–205, 2024.

[34] L. Ma, H. Liu, L. Zhou, C. Yang, W. Dai, and G. Wang, "Security control for multi-time-scale CPSs under DoS attacks: An improved dynamic event-triggered mechanism," *IEEE Trans. Netw. Sci. Eng.*, vol. 9, no. 3, pp. 1813–1826, May/Jun. 2022.

[35] F. Liu, L. Wu, Q. Liu, and D. Sidorov, "Dynamic-memory event-triggered secure control for cyber-physical power systems under hybrid attacks," *IEEE Trans. Netw. Sci. Eng.*, vol. 12, no. 5, pp. 3850–3863, Sep./Oct. 2025.

[36] Y. Zhao, C. Zhou, Y.-C. Tian, Y. Qin, and X. Hu, "l_2 gain secure control of cyber-physical systems under fast time-varying cyber attacks," *IEEE Trans. Netw. Sci. Eng.*, vol. 9, no. 2, pp. 648–659, Mar./Apr. 2022.

[37] Y. Zhang, L. Ma, G. Wang, C. Yang, L. Zhou, and W. Dai, "Observer-based control for the two-time-scale cyber-physical systems: The dual-scale DoS attacks case," *IEEE Trans. Netw. Sci. Eng.*, vol. 8, no. 4, pp. 3369–3379, Oct.–Dec. 2021.

[38] X. Guan, Y. Hu, and K. Peng, "Stackelberg-game-based sliding mode fault-tolerant secure control for cyber-physical systems against jamming attacks and multiple physical intermittent faults," *IEEE Trans. Netw. Sci. Eng.*, vol. 11, no. 5, pp. 4344–4357, Sep./Oct. 2024.

[39] J. Ma, H. Zhang, J. Zhang, and X. Guo, "Event-based adaptive fault-tolerant control for nonlinear cyber-physical systems via intermittent available signals," *IEEE Trans. Autom. Sci. Eng.*, vol. 22, pp. 19850–19859, 2025.

[40] Y. Gao, J. Ma, J. Wang, and Y. Wu, "Event-triggered adaptive fixed-time secure control for nonlinear cyber-physical system with false data-injection attacks," *IEEE Trans. Circuits Syst. II: Exp. Briefs*, vol. 70, no. 1, pp. 316–320, Jan. 2023.

[41] L. Lyu, C. Chen, S. Zhu, X. Wen, and X. Guan, "Sensing aware opportunistic transmissions for situation monitoring in industrial network systems," in *Proc. IEEE Glob. Commun. Conf.*, 2019, pp. 1–6.

[42] G. Pang, W. Liu, D. Niyato, B. Vucetic, and Y. Li, "Communication-control codesign for large-scale wireless networked control systems," *IEEE J. Sel. Areas Commun.*, vol. 43, no. 10, pp. 3295–3312, Oct. 2025.

[43] T. Huang et al., "Hirail: Core-agnostic deterministic networks for long-distance time-sensitive IIoT applications," *IEEE Internet Things J.*, vol. 11, no. 10, pp. 17198–17209, May 2024.

[44] L. Lyu et al., "AGV-assisted adaptive cooperative transmission for state estimation in industrial IoT systems," *IEEE Trans. Veh. Technol.*, vol. 74, no. 2, pp. 2390–2405, Feb. 2025.

[45] Y. Yan, Y. Wang, W. Ni, and D. Niyato, "Joint beamforming design for multi-functional RIS-aided uplink communications," *IEEE Commun. Lett.*, vol. 27, no. 10, pp. 2697–2701, Oct. 2023.

[46] J. Huang, T. Yu, F. Yang, S. Zhang, W. Jiang, and D. Niyato, "AoI-aware resource allocation with interference avoidance for ultradense industrial Internet of Things networks," *IEEE Internet Things J.*, vol. 11, no. 17, pp. 28787–28797, Sep. 2024.

[47] L. Lyu et al., "Adaptive edge sensing for industrial IoT systems: Estimation task offloading and sensor scheduling," *IEEE Internet Things J.*, vol. 10, no. 1, pp. 391–402, Jan. 2023.

[48] R. Xie et al., "Priority-aware task scheduling in computing power network-enabled edge computing systems," *IEEE Trans. Netw. Sci. Eng.*, vol. 12, no. 4, pp. 3191–3205, Jul./Aug. 2025.

[49] T. Z. H. Ernest and A. S. Madhukumar, "Timeliness-aware computation offloading strategies for IIoT networks," *IEEE Trans. Netw. Sci. Eng.*, vol. 12, no. 5, pp. 4239–4254, Sep./Oct. 2025.

[50] C. Xu et al., "Optimal status updates for minimizing age of correlated information in IoT networks with energy harvesting sensors," *IEEE Trans. Mobile Comput.*, vol. 23, no. 6, pp. 6848–6864, Jun. 2024.

[51] J. Wen, J. Kang, D. Niyato, Y. Zhang, and S. Mao, "Sustainable diffusion-based incentive mechanism for generative AI-driven digital twins in industrial cyber-physical systems," *IEEE Trans. Ind. Cyber- Phys. Syst.*, vol. 3, pp. 139–149, 2025.

[52] L. Lyu, C. Chen, S. Zhu, and X. Guan, "5G enabled codesign of energy-efficient transmission and estimation for industrial IoT systems," *IEEE Trans. Ind. Informat.*, vol. 14, no. 6, pp. 2690–2704, Jun. 2018.

[53] L. Chen, H. Liang, X. Zhang, and T. Li, "Distributed guaranteed-performance consensus of networked systems without involving the feasibility condition: A hierarchical algorithm," *IEEE Trans. Netw. Sci. Eng.*, vol. 12, no. 4, pp. 2445–2457, Jul./Aug. 2025.

[54] S. M. Nagarajan, G. G. Devarajan, A. S. Mohammed, T. Ramana, and U. Ghosh, "Intelligent task scheduling approach for IoT integrated healthcare cyber physical systems," *IEEE Trans. Netw. Sci. Eng.*, vol. 10, no. 5, pp. 2429–2438, Sep./Oct. 2023.

[55] Z. Cui, Z. Zhang, Z. Hu, S. Geng, and J. Chen, "A many-objective optimization based intelligent high performance data processing model for cyber-physical-social systems," *IEEE Trans. Netw. Sci. Eng.*, vol. 9, no. 6, pp. 3825–3834, Nov./Dec. 2022.

[56] X. Chen, W. Liang, J. Xu, C. Wang, K.-C. Li, and M. Qiu, "An efficient service recommendation algorithm for cyber-physical-social systems," *IEEE Trans. Netw. Sci. Eng.*, vol. 9, no. 6, pp. 3847–3859, Nov./Dec. 2022.

[57] H. Mughal, M. Bilal, U. Ghosh, G. Srivastava, and S. C. Shah, "Efficient allocation of resource-intensive mobile cyber-physical social system applications on a heterogeneous mobile ad hoc cloud," *IEEE Trans. Netw. Sci. Eng.*, vol. 9, no. 3, pp. 958–969, May/Jun. 2022.

[58] L. Chen et al., "Impact of cascading failure on power distribution and data transmission in cyber-physical power systems," *IEEE Trans. Netw. Sci. Eng.*, vol. 11, no. 2, pp. 1580–1590, Mar./Apr. 2024.

[59] Z. Dong and M. Tian, "Modeling and vulnerability analysis of spatially embedded heterogeneous cyber-physical systems with functional dependency," *IEEE Trans. Netw. Sci. Eng.*, vol. 8, no. 4, pp. 3404–3416, Oct.–Dec. 2021.

[60] P. Qin, Y. Fu, K. Wu, J. Zhang, X. Wu, and X. Zhao, "Packet routing and energy cooperation for RTU satellite-terrestrial multi-hop network in remote cyber-physical power system," *IEEE Trans. Netw. Sci. Eng.*, vol. 11, no. 4, pp. 3585–3597, Jul./Aug. 2024.

[61] Z. Peng, Y. Zhang, G. Wen, J. Wang, and T. Huang, "Resilient output consensus to cyber-attacks in continuous-time cyber-physical systems," *IEEE Trans. Netw. Sci. Eng.*, vol. 10, no. 4, pp. 2190–2200, Jul./Aug. 2023.

[62] J. Li, D. Yu, W. Ma, J. J. R. Liu, and Y.-J. Liu, "Cooperative control of air–ground swarms under DoS attacks via cloud–Fog computing," *IEEE Trans. Netw. Sci. Eng.*, vol. 11, no. 5, pp. 4278–4292, Sep./Oct. 2024.

[63] Y. Li et al., "A correlated data-driven collaborative beamforming approach for energy-efficient IoT data transmission," *IEEE Internet Things J.*, vol. 12, no. 12, pp. 22443–22462, Jun. 2025.

[64] D. Kim, H. Jung, I.-H. Lee, and D. Niyato, "Novel resource allocation algorithm for IoT networks with multicarrier noma," *IEEE Internet Things J.*, vol. 11, no. 18, pp. 30354–30367, Sep. 2024.

[65] M. Katwe, K. Singh, B. Clerckx, and C. P. Li, "Rate splitting multiple access for sum-rate maximization in IRS aided uplink communications," *IEEE Trans. Wireless Commun.*, vol. 22, no. 4, pp. 2246–2261, Apr. 2023.

[66] C. Xu, M. Wu, Y. Xu, and Y. Fang, "Uplink low-power scheduling for delay-bounded industrial wireless networks based on imperfect power-domain NOMA," *IEEE Syst. J.*, vol. 14, no. 2, pp. 2443–2454, Jun. 2020.

[67] D. Li, J. Li, D. Niyato, W. Feng, and W. Jiang, "Deep energy-efficient optimization network for URLLC over cell-free massive MIMO," *IEEE Internet Things J.*, vol. 12, no. 12, pp. 20973–20987, Jun. 2025.

[68] X. Jiao et al., "Energy-aware minimum delay broadcast scheduling for SIC-enabled wireless-powered IoT," *IEEE Trans. Ind. Informat.*, vol. 20, no. 4, pp. 5263–5273, Apr. 2024.

[69] P. Zhang, H. Tian, P. Zhao, and S. Fan, "Context-aware mobile edge resource allocation in OFDMA downlink system," *IEEE Trans. Netw. Sci. Eng.*, vol. 10, no. 5, pp. 2755–2768, Sep./Oct. 2023.

[70] L. Lyu et al., "Dyna mics-aware and beamforming-assisted transmission for wireless control scheduling," *IEEE Trans. Wireless Commun.*, vol. 17, no. 11, pp. 7677–7690, Nov. 2018.

[71] Y.-J. Yu, Y.-C. Wang, and C.-H. Fan, "Control period adaptation and resource allocation for joint uplink and downlink in NB-IoT networks," *IEEE Internet Things J.*, vol. 11, no. 9, pp. 16746–16757, May 2024.

[72] S. F. Kimaryo and K. Lee, "Uplink and downlink capacity maximization of a P2P DMA-based communication system," *IEEE Trans. Wireless Commun.*, vol. 23, no. 10, pp. 14037–14051, Oct. 2024.
[73] K. Li, P. Zhu, Y. Wang, F.-C. Zheng, and X. You, "Joint uplink and downlink resource allocation toward energy-efficient transmission for URLLC," *IEEE J. Sel. Areas Commun.*, vol. 41, no. 7, pp. 2176–2192, Jul. 2023.
[74] L. Zhang, Y. Zhang, and J. Zheng, "Deep reinforcement learning based joint uplink and downlink resource allocation for URLLC," *IEEE Trans. Veh. Technol.*, vol. 74, no. 4, pp. 6048–6063, Apr. 2025.
[75] X. Chen et al., "Downlink and uplink cooperative joint communication and sensing," *IEEE Trans. Veh. Technol.*, vol. 73, no. 8, pp. 11318–11332, Aug. 2024.
[76] X. Guo, B. Li, J. Wu, R. Zhang, and X. Cheng, "Joint uplink and downlink NOMA for UAV relaying network with multi-pair users," *IEEE Trans. Wireless Commun.*, vol. 23, no. 12, pp. 18549–18562, Dec. 2024.
[77] X. Chen, Z. Feng, Z. Wei, J. A. Zhang, X. Yuan, and P. Zhang, "Concurrent downlink and uplink joint communication and sensing for 6 G networks," *IEEE Trans. Veh. Technol.*, vol. 72, no. 6, pp. 8175–8180, Jun. 2023.
[78] J. Zhou, Y. Chen, C. Zhou, Y. Sun, and C. Tellambura, "Joint uplink and downlink rate splitting for fog-computing-enabled internet of medical things," *IEEE Internet Things J.*, vol. 11, no. 23, pp. 37872–37884, Dec. 2024.
[79] X. Xia et al., "Joint uplink power control, downlink beamforming, and mode selection for secrecy cell-free massive MIMO with network-assisted full duplexing," *IEEE Syst. J.*, vol. 17, no. 1, pp. 720–731, Mar. 2023.
[80] L. Schenato, B. Sinopoli, M. Franceschetti, K. Poolla, and S. S. Sastry, "Fo undations of control and estimation over lossy networks," *Proc. IEEE*, vol. 95, no. 1, pp. 163–187, Jan. 2007.
[81] B. Sinopoli, L. Schenato, M. Franceschetti, K. Poolla, M. Jordan, and S. S. Sastry, "Kalman filtering with intermittent observations," *IEEE Trans. Autom. Control*, vol. 49, no. 9, pp. 1453–1464, Sep. 2004.
[82] C. Ramesh, H. Sandberg, and K. H. Johansson, "Design of state-based schedulers for a network of control loops," *IEEE Trans. Autom. Control*, vol. 58, no. 8, pp. 1962–1975, Aug. 2013.
[83] W. R. Ghanem, V. Jamali, and R. Schober, "Optimal resource allocation for multi-user OFDMA-URLLC MEC systems," *IEEE Open J. Commun. Soc.*, vol. 3, pp. 2005–2023, 2022.
[84] H. Liu and L. Lyu, "Co-design of transmission and control in industrial IoT systems," in *Proc. IEEE/CIC Int. Conf. Commun. China*, 2024, pp. 615–620.
[85] C. Zhang, M. Dong, and B. Liang, "Ultra-low-complexity algorithms with structurally optimal multi-group multicast beamforming in large-scale systems," *IEEE Trans. Signal Process.*, vol. 71, pp. 1626–1641, 2023.
[86] D. Feng, L. Lu, Y. Yuan-Wu, G. Y. Li, G. Feng, and S. Li, "Device-to-device communications underlaying cellular networks," *IEEE Trans. Commun.*, vol. 61, no. 8, pp. 3541–3551, Aug. 2013.
[87] F. Wang, J. Chen, and F. Liu, "KeyFrame generation method via improved clustering and silhouette coefficient for video summarization," *J. Web Eng.*, vol. 20, no. 1, pp. 147–170, Jan. 2021.
[88] K. P. Sinaga and M. S. Yang, "Unsupervised K-means clustering algorithm," *IEEE Access*, vol. 8, pp. 80716–80727, 2020.
[89] Z. Zhang et al., "Joint user grouping, version selection, and bandwidth allocation for live video multicasting," *IEEE Trans. Commun.*, vol. 70, no. 1, pp. 350–365, Jan. 2022.

Ling Lyu (Member, IEEE) received the B.Eng. degree in telecommunication engineering from Jinlin University, Changchun, China, in 2013, and the Ph.D. degree in control theory and control engineering from Shanghai Jiao Tong University, Shanghai, China, in 2019. In 2019, she joined Dalian Maritime University, Dalian, China, where she is currently an Associate Professor with the School of Information Science and Technology. From 2017 to 2018, she was a Visiting Student with the University of Waterloo, Waterloo, ON, Canada. Her research interests include wireless sensor and actuator network and application in industrial automation, the joint design of communication and control in industrial cyber-physical systems, estimation and control over lossy wireless networks, and control-aware integrated sensing and communication.

Haitian Liu received the B.E. and M.S. degrees from the School of Information Science and Technology, Dalian Maritime University, Dalian, China, in 2021 and 2025, respectively. His research interest includes resource allocation and wireless network control.

Yanpeng Dai (Member, IEEE) received the B.Eng. degree in telecommunication engineering from Shandong Normal University, Jinan, China, in 2014, and the Ph.D. degree in communication and information systems from Xidian University, Xi'an, China, in 2020. He is currently an Associate Professor with the School of Information Science and Technology, Dalian Maritime University, Dalian, China. He was a Visiting Student with the University of Waterloo, Waterloo, ON, Canada. His research interests include resource management and interference coordination for heterogeneous wireless networks and maritime communication systems.

Nan Cheng (Senior Member, IEEE) received the B.E. and M.S. degrees from the Department of Electronics and Information Engineering, Tongji University, Shanghai, China, in 2009 and 2012, respectively, and the Ph.D. degree from the Department of Electrical and Computer Engineering, University of Waterloo, Waterloo, ON, Canada, in 2016. From 2017 to 2019, he was a Postdoctoral Fellow with the Department of Electrical and Computer Engineering, University of Toronto, Toronto, ON, Canada. He is currently a Professor with the State Key Laboratory of ISN and with School of Telecommunications Engineering, Xidian University, Shaanxi, China. He has authored or coauthored more than 90 journal papers in IEEE Transactions and other top journals. His research interests include B5G/6 G, AI-driven future networks, and space-air-ground integrated network. He is also an Associate Editors for IEEE TRANSACTIONS ON VEHICULAR TECHNOLOGY, IEEE OPEN JOURNAL OF THE COMMUNICATIONS SOCIETY, and *Peer-to-Peer Networking and Applications*. He is/was the Guest Editors of several journals.

Cailian Chen (Senior Member, IEEE) received the B.Eng. and M.Eng. degrees in automatic control from Yanshan University, Qinhuangdao, China, in 2000 and 2002, respectively, and the Ph.D. degree in control and systems from the City University of Hong Kong, Hong Kong, SAR, China, in 2006. Since 2008, she has been with the Department of Automation, Shanghai Jiao Tong University, Shanghai, China. She is currently a Distinguished Professor. She has authored three research monographs and more than 100 refereed international journal articles. She is also the Inventor of more than 30 patents. Her research interests include industrial wireless networks and computational intelligence and the Internet of Vehicles. Dr. Chen was the recipient of the prestigious IEEE Transactions on Fuzzy Systems Outstanding Paper Award in 2008, IEEE TCCPS Industrial Technical Excellence Award in 2022, the five conference Best Paper awards, N2Women Star in Computer Networking and Communications in 2022, the Second Prize of National Natural Science Award from the State Council of China in 2018, First Prize of Natural Science Award from The Ministry of Education of China in 2006 and 2016, respectively, and First Prize of Technological Invention of Shanghai Municipal, China, in 2017, and was also honored "National Outstanding Young Researcher" by NSF of China in 2020, "Changjiang Young Scholar" in 2015, and China Young Women Scientists Award in 2023. She has been actively involved in various professional services. She is a Distinguished Lecturer of IEEE VTS. She is the Deputy Editor of *National Science Open* and an Associate Editor for IEEE TRANSACTIONS ON VEHICULAR TECHNOLOGY and *IET Cyber-Physical Systems: Theory & Applications*.

Xinping Guan (Fellow, IEEE) is currently a Chair Professor with Shanghai Jiao Tong University, Shanghai, China, where he is also the Dean of the School of Electronic, Information and Electrical Engineering and the Director with the Key Laboratory of Systems Control and Information Processing, Ministry of Education of China. Before that, he was the Executive Director of Office of Research Management with Shanghai Jiao Tong University and a Full Professor and the Dean of Electrical Engineering with Yanshan University, Qinhuangdao, China. He has authored and/or coauthored five research monographs, more than 200 papers in peer-reviewed journals, and numerous conference papers. His research interests include industrial network systems, smart manufacturing, and underwater networks. He has finished/been working on more than 20 National Key Projects, as a Principal Investigator. He is also the Leader with prestigious Innovative Research Team, National Natural Science Foundation of China (NSFC). He is an Executive Committee Member of Chinese Automation Association Council and Chinese Artificial Intelligence Association Council. Dr. Guan was the recipient of the First Prize of Natural Science Award from the Ministry of Education of China in 2006 and 2016, the Second Prize of the National Natural Science Award of China in 2008 and 2018, the "IEEE Transactions on Fuzzy Systems Outstanding Paper Award" in 2008, and IEEE TCCPS Industrial Technical Excellence Award in 2022. He was also honored "National Outstanding Youth" by NSF of China, "Changjiang Scholar" by the Ministry of Education of China and "State-Level Scholar" of "New Century Bai Qianwan Talent Program" of China.

Xuemin (Sherman) Shen (Fellow, IEEE) received the Ph.D. degree in electrical engineering from Rutgers University, New Brunswick, NJ, USA, in 1990. He is currently a University Professor with the Department of Electrical and Computer Engineering, University of Waterloo, Waterloo, ON, Canada. His research interests include network resource management, wireless network security, Internet of Things, 5G and beyond, and vehicular networks. Dr. Shen was the recipient of the "West Lake Friendship Award" from Zhejiang Province in 2023, President's Excellence in Research from the University of Waterloo in 2022, Canadian Award for Telecommunications Research from the Canadian Society of Information Theory (CSIT) in 2021, the R.A. Fessenden Award in 2019 from IEEE, Canada, Award of Merit from the Federation of Chinese Canadian Professionals (Ontario) in 2019, James Evans Avant Garde Award in 2018 from the IEEE Vehicular Technology Society, Joseph LoCicero Award in 2015 and Education Award in 2017 from the IEEE Communications Society (ComSoc), and Technical Recognition Award from Wireless Communications Technical Committee (2019), AHSN Technical Committee (2013), the Excellent Graduate Supervision Award in 2006 from the University of Waterloo, and the Premier's Research Excellence Award (PREA) in 2003 from the Province of Ontario, Canada. He is/was the General Chair for the 6G Global Conference'23, and ACM Mobihoc'15, Technical Program Committee Chair/Co-Chair for IEEE Globecom'24, 16 and 07, IEEE Infocom'14, IEEE VTC'10 Fall, and the Chair for the IEEE ComSoc Technical Committee on Wireless Communications. He is also the Past President of the IEEE ComSoc, Vice President for Technical & Educational Activities, Vice President for Publications, Member-at-Large on the Board of Governors, Chair of the Distinguished Lecturer Selection Committee, and Member of IEEE Fellow Selection Committee of the ComSoc. He was the Editor-in-Chief of the IEEE IoT JOURNAL, IEEE NETWORK, and PPNA. He is also a registered Professional Engineer of Ontario, Canada, an Engineering Institute of Canada Fellow, a Canadian Academy of Engineering Fellow, a Royal Society of Canada Fellow, a Chinese Academy of Engineering Foreign Member, and an International Fellow of the Engineering Academy of Japan.